INSTITUTO POTOSINO DE INVESTIGACIÓN CIENTÍFICA Y TECNOLÓGICA, A. C.

POSGRADO EN CIENCIAS APLICADAS

Optimization of Entanglement using Genetic Algorithms

Tesis que presenta

Jorge Carlos Navarro Muñoz

Para obtener el grado de

Doctor en Ciencias Aplicadas

En la opción de

Nanociencias y Nanotecnología

Director de Tésis:

Dr. Román López-Sandoval

San Luis Potosí, S.L.P., Febrero de 2012

La tesis "**Optimization of Entanglement using Genetic Algorithms**" presentada para obtener el Grado de Doctor en Ciencias Aplicadas en la opción de Nanociencias y Nanotecnología fue elaborada por **Jorge Carlos Navarro Muñoz** y aprobada el **13 de Febrero de 2012** por los suscritos, designados por el Colegio de Profesores de la División de Materiales Avanzados del Instituto Potosino de Investigación Científica y Tecnológica, A.C.

Dr. Román López Sandoval
Director de la tesis

Dr. José Luis Rodríguez López

Dr. José Luis Ricardo Chávez

Dr. Braulio Gutiérrez Medina

Dr. Raúl Garibay Alonso

Esta tesis fue elaborada en la División de Materiales Avanzados del Instituto Potosino de Investigación Científica y Tecnológica, A.C., bajo la supervisión del doctor Román López Sandoval.

Durante la realización del trabajo el autor recibió una beca académica del Consejo Nacional de Ciencia y Tecnología (204220), así como del Apoyo al Fomento de formación de Doctores en Ciencias (52721) por parte de la misma institución. Así mismo, recibió un apoyo de parte del Comité de Becas del Instituto Potosino de Investigación Científica y Tecnológica, A.C..

IPICYT

Instituto Potosino de Investigación Científica y Tecnológica, A.C.

Acta de Examen de Grado

El Secretario Académico del Instituto Potosino de Investigación Científica y Tecnológica, A.C., certifica que en el Acta 038 del Libro Primero de Actas de Exámenes de Grado del Programa de Doctorado en Ciencias Aplicadas en la opción de Nanociencias y Nanotecnología está asentado lo siguiente:

En la ciudad de San Luis Potosí a los 13 días del mes de febrero del año 2012, se reunió a las 17:10 horas en las instalaciones del Instituto Potosino de Investigación Científica y Tecnológica, A.C., el Jurado integrado por:

Dr. José Luis Rodríguez López	**Presidente**	**IPICYT**
Dr. Raúl Garibay Alonso	**Secretario**	**UAdeC**
Dr. Braulio Gutiérrez Medina	**Sinodal**	**IPICYT**
Dr. José Luis Ricardo Chávez	**Sinodal**	**IPICYT**
Dr. Román López Sandoval	**Sinodal**	**IPICYT**

a fin de efectuar el examen, que para obtener el Grado de:

DOCTOR EN CIENCIAS APLICADAS
EN LA OPCIÓN DE NANOCIENCIAS Y NANOTECNOLOGÍA

sustentó el C.

Jorge Carlos Navarro Muñoz

sobre la Tesis intitulada:

Optimization of Entanglement using Genetic Algorithms

que se desarrolló bajo la dirección de

Dr. Román López Sandoval

El Jurado, después de deliberar, determinó

APROBARLO

Dándose por terminado el acto a las 18:25 horas, procediendo a la firma del Acta los integrantes del Jurado. Dando fe el Secretario Académico del Instituto.

A petición del interesado y para los fines que al mismo convengan, se extiende el presente documento en la ciudad de San Luis Potosí, S.L.P., México, a los 13 días del mes de febrero de 2012.

Dr. Marcial Bonilla Marín
Secretario Académico

INSTITUTO POTOSINO
DE INVESTIGACIÓN
CIENTÍFICA Y TECNOLÓGICA, A.C.
IPICYT
SECRETARIA ACADEMICA

Mtra. Ivonne Lizette Cuevas Vélez
Jefa del Departamento del Posgrado

To p!

Acknowledgements

This work would not be possible without the help of many people, particularly Pily and my parents. My utmost gratitude to them.

Contents

List of Figures

List of Tables

Resumen

En tiempos recientes la búsqueda de un modelo más general de computación derivó finalmente en el concepto de la computadora cuántica, un esquema de procesamiento de información basado totalmente en fenómenos cuánticos.

Esto, a su vez, ha propiciado el estudio de nuevos recursos tales como el *Entanglement*, que se define como un tipo especial de correlación que tiene lugar a nivel cuántico.

En el presente trabajo, se estudia la optimización numérica de la Concurrencia –una medida de Entanglement– a primeros vecinos en redes bipartitas de una y dos dimensiones, así como no-bipartitas en algunas redes de dos dimensiones. Los resultados muestran que la Concurrencia de las redes optimizadas es considerablemente más alta que en aquellas donde no hubo optimización. En el caso de las cadenas unidimensionales, la Concurrencia incrementa de manera notable cuando el sistema presenta el fenómeno de dimerización. Más aún, la optimización más alta de Concurrencia en redes de dos dimensiones bipartitas y no-bipartitas se alcanza cuando las estructuras tienden a romperse en subsistemas más pequeños, los cuales se encuentran arreglados en configuraciones geométricamente distinguibles.

Palabras Clave: Computación Cuántica, Entanglement, Concurrencia, Algoritmos Genéticos, Amarre-fuerte.

Abstract

In recent times the research to find a more general model of computation ultimately led to the concept of the quantum computer, an information-processing scheme based entirely on quantum phenomena.

This, in turn, has led to the study of new resources such as *Entanglement*, which is defined as a special kind of correlation found only at quantum scales.

In the present work, we study the numerical optimization of nearest-neighbor Concurrence –a measurement of entanglement–, of bipartite one- and two-dimensional lattices, as well as non-bipartite two-dimensional lattices. Results show that the Concurrence of the optimized lattice structures is considerably higher than that of non-optimized systems. In the case of one-dimensional chains, the Concurrence increases remarkably when the system begins to dimerize. Moreover, the optimization of Concurrence in two-dimensional bipartite and non-bipartite lattices is achieved when the structures break into smaller subsystems, which are arranged in geometrically distinguishable configurations.

Key Words: Quantum Computation, Entanglement, Concurrence, Genetic Algorithms, Tight-binding.

Chapter 1

Context

1.1 The Classical Computer

1.1.1 A brief introduction

"We were born in a sea of information". A phrase that could probably come from a science-fiction movie decades ago, is today a reality. The development of the transistor in the 1950's and many other sciences has made it possible for the so-called "personal computer" to be ubiquitous. People communicate by e-mail or SMS; chats with friends; plays video games online; writes blogs and perform bank operations over the web on a daily basis. They also run distributed software with scientific purposes, mantain business databases and, sometimes, write PHD dissertations. But technology has not found its way exclusively on personal computers: it has also permeated onto society in the form of cell phones, music players, TV's and several daily-life objects.

The processing of this mammoth amount of data is performed by means of binary operations for historic reasons. In 1937, Claude Shannon, considered as the father of information theory, proved in his master's thesis [6] that the logic used to relate numbers in their binary representation (i.e. boolean algebra) could be used to simplify the electromechanical relays used at that time by telephone routers. Reversely, he used the same concept to prove that the relays could be employed to perform boolean algebra, providing in the process an invaluable tool to forecoming engineers interested in building "processing machines".

The kind of data with this characteristic (that is, that can be in one of only two distinct states) is called a *bit*, and while the first ancestors of modern computation —Babbage's Difference Engine and the ENIAC— still worked with the decimal system, machines designed to work on binary are

simpler and easier to build. Having only two states makes them resilient to noise and thus more reliable when moving data.

The Z3 (built by another pioneer, Konrad Zuse), was the first computer that used the binary system to perform calculations. In 1998, three years after Zuse's death, it was proved that Z3 is Turing-complete.

A year prior to the publication of Shannon's thesis, Alan Turing had made a serious and important contribution to computer science. He defined the *concept*, commonly known nowadays as a Turing Machine, which comprehends a set of ideas (an infinite *tape* divided in cells containing a symbol from a finite alphabet; a *head* with the ability of storing and retrieving symbols in the tape; a *table* where instructions tell the machine to perform actions like moving the head or writing a symbol, and finally a *state register* which tells the state of the machine) that came to be the base of present-day algorithms. A device classified as Turing-complete is such that can be emulated by a general or *Universal* Turing machine. Nor the Z3 —or any computer—, of course, posseses an infinite amount of memory.

Along with Alonzo Church, Stephen Kleene and J. B. Rosse, Turing's theories are summed in an ongoing set of *thesis* which try to define what kind of algorithmic process can be simulated by different approaches (the Turing Machine being the prominent one). By the end of the 1960's, the thesis was concerned with how *efficiently* can an algorithmic process be simulated with a Turing Machine.

"Efficiently" means that the time for solving a certain problem will not grow exponentially with its size (alternatively, it may also mean that a PhD student will finish all her simulations before the graduation date). Problems have been categorized into many kinds, some of which are thought not to have an efficient way to be solved.

A formidable challenge to the well-stablished Turing Machine theses came by the mid 70's when Robert Solovay and Volker Strassen proposed a probabilistic method that determines whether a number is prime [8]. This means that, eventhough this particular algorithm may fail, such probability can be reduced arbitrarily with the number of iterations. Although these "primality tests" have found quick (though not *quicker* than their probabilistic counterpart) deterministic algorithms that run in polynomial times (i.e. the Agrawal, Kayal y Saxena, AKS algorithm), the Solovay-Strassen algorithm proved that more general theses were still to be found, with the result of the inclusion of randomness in yet another thesis: "A *probabilistic* Turing machine can efficiently simulate any realistic model of computation".

Fast forward to the present day. It is know that microchips follow the so-called "Moore's Law", which states that the amount of transistors in an

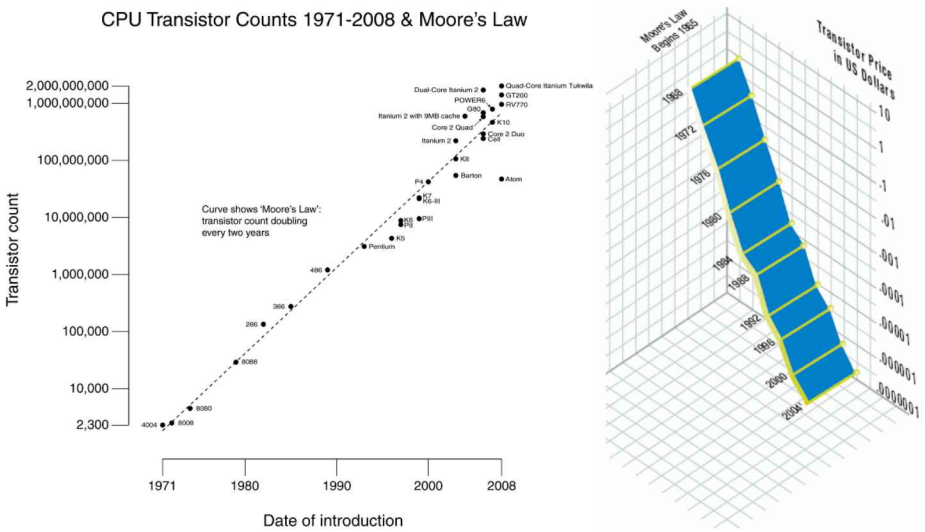

(a) Number of transistors by CPU

(b) Price, in dollars, by transistor

Figure 1.1: Creative Commons, Wgsimon; Copyright 2005 Intel Corporation

integrated circuit doubles each two years. Whether Moore's Law truthfully predicts the industry's developments or the industry adapts itself in order to follow the Law is debatable. The fact is that Moore's Law has been followed, at least until now.

It is evident, however, that Moore's Law is beginning to see bumps in the road ahead. This is due to the ever smaller components found in each new generation of CPUs. For example, when companies tried to manufacture microchips whose transistors featured a gate of only 45 nm, they realized that traditional processes would not be enough to cope with the inevitable leak of electrons. The combination of such a small feature as well as the material employed enabled electrons to tunnel the potential barrier that separeted them from the channel. This was eventually accounted for using another kind of dielectric (see [1]), but it is clear that quantum effects are starting to play a crucial role in technology. At the time of writing, the state-of-the-art processors have transistors with features of up to 32 nm.

1.2 The Quantum Computer

Even before the limitations of current approaches to manufacturing small components became evident, the idea had been proposed [3] of developing an information-processing device based entirely on quantum

phenomena.

Motivated by these issues, David Deutsch wondered whether the laws of physics could be used to derive an even stronger version of the Church-Turing thesis [2]. In particular, Deutsch attempted to define a computational device that would be capable of efficiently simulate an arbitraty physical system. Because the laws of physics are ultimately quantun mechanical, he was naturally led to consider computing devices based on the principles of quantum mechanics.

Though the concept of quantum computer is relatively new, there are already some proposals in which these concepts are applied with exciting new results: algorithms that perform much better than their classic counterparts, stronger cryptography and new phenomena such as quantum teleportation.

Much work, however, is still needed to harness all the potential of quantum computation.

1.2.1 Qubits

Just like a classic bit has a definite state —0 or 1—, a quantum bit, or *qubit*, is simply a quantum system with two distinguishable states, such as the two levels of a $\frac{1}{2}$ spin particle; the ground and first excited state of an atom, or the vertical or horizontal polarization of a photon. Dirac notation is usually employed, and the two systems are labeled commonly $|0\rangle$ and $|1\rangle$.

The most remarkable —and crucial— feature of qubits is that they can be found in a *superposition* of the two states. This means that it is possible to form linear combinations of states. A general state of a qubit is thus:

$$|\psi\rangle = \alpha|0\rangle + \beta|1\rangle. \tag{1.1}$$

When a qubit is measured, the result can be either the state $|0\rangle$ with probability $|\alpha|^2$ or the state $|1\rangle$ with probability $|\beta|^2$ —so as to make the sum of probabilities equal to 1—. A qubit can be pictured as a unitary vector in a two-dimensional space (although, as the state's coefficients are, in general, complex numbers, it can be seen rather as a *sphere* with radius 1).

For the case of two qubits, it is clear that four different states are possible. Such a system can be represented as:

$$|\psi_{\text{dos qubits}}\rangle = \alpha|00\rangle + \beta|01\rangle + \gamma|10\rangle + \delta|11\rangle. \tag{1.2}$$

The matrix notation can be employed too, with each row indicating the coefficient of each state, ordered:

$$\alpha|00\rangle + \beta|01\rangle + \gamma|10\rangle + \delta|11\rangle = \begin{pmatrix} \alpha \\ \beta \\ \gamma \\ \delta \end{pmatrix}. \tag{1.3}$$

In Dirac's notation, the first state to the left represents the first qubit, that is, the state $|01\rangle$ can be read as "the state whose first qubit is in the state $|0\rangle$ while the second is in the state $|1\rangle$".

Operators

Mathematically, qubits can be manipulated using *operators*, which are any unitary matrices. A unitary matrix A satisfy $A^\dagger A = I$, where $A^\dagger$ is the *adjoint*, *Hermitian* or conjugate-transpose of A.

For example, the following operator, $\mathbf{CNOT}$ is a two-qubit operator which switches the second qubit's state if the first one is in the state $|1\rangle$:

$$\begin{pmatrix} 1 & 0 & 0 & 0 \\ 0 & 1 & 0 & 0 \\ 0 & 0 & 0 & 1 \\ 0 & 0 & 1 & 0 \end{pmatrix}. \tag{1.4}$$

It can be easily seen that $(\mathbf{CNOT})(\mathbf{CNOT}^\dagger) = \mathbf{I}$.

Measurement

Although the evolution of a quantum system by means of unitary operators implies a closed system, there must be some manner to obtain useful information once the desired manipulations have finished. *Measurement* is performed by means of a set of operators $\{M_m\}$, whose index m represents each possible state in the outcome. If a system's state before measurement is $|\psi\rangle$, then the probability of obtaining result m after measurement is given by

$$p(m) = \langle\psi|M_m^\dagger M_m|\psi\rangle, \tag{1.5}$$

and the system's state after measurement becomes

$$\frac{M_m|\psi\rangle}{\sqrt{\langle\psi|M_m^\dagger M_m|\psi\rangle}}. \tag{1.6}$$

To ensure that the sum of probabilities equals 1, measurement operators must satisfy the completeness equation

$$\sum_m M_m^\dagger M_m = I. \tag{1.7}$$

The system can be measured progressively, one qubit at a time, in the desired order. It is possible, for example, to measure a system's first qubit from equation (1.2). The probability that such measurement yields the state $|0\rangle$ is $|\alpha|^2 + |\beta|^2$, in which case the system could be described as

$$|\psi'\rangle = \frac{\alpha|00\rangle + \beta|01\rangle}{\sqrt{|\alpha|^2 + |\beta|^2}} \tag{1.8}$$

where the denominator has been introduced for normalization (although only two states are accessible, the sum of their probabilities must sum 1 again). If instead of measuring the first qubit the second one is measured, the state $|1\rangle$ would be observed with probability $|\beta|^2 + |\delta|^2$, leaving the system in the state

$$|\psi'\rangle = \frac{\beta|01\rangle + \delta|11\rangle}{\sqrt{|\beta|^2 + |\delta|^2}}. \tag{1.9}$$

As a quick example, we can define two operators for one qubit: $M_0 = |0\rangle\langle 0|$ y $M_1 = |1\rangle\langle 1|$. In matrix notation these are:

$$M_0 \equiv \begin{array}{c|cc} & \langle 0| & \langle 1| \\ \hline |0\rangle & 1 & 0 \\ |1\rangle & 0 & 0 \end{array} \qquad M_1 \equiv \begin{array}{c|cc} & \langle 0| & \langle 1| \\ \hline |0\rangle & 0 & 0 \\ |1\rangle & 0 & 1 \end{array}. \tag{1.10}$$

It can be easily seen that both operators are hermitic and satisfy the completeness equation. Note also that $M_m^\dagger M_m = M_m^2 = M_m$.

For a general qubit $|\psi\rangle = \alpha|0\rangle + \beta|1\rangle$, the probability to measure the state 0 is

$$\begin{aligned} p(0) &= \langle\psi|M_0^\dagger M_0|\psi\rangle = \langle\psi|M_0|\psi\rangle \\ &= (a^*\langle 0| + b^*\langle 1|)\,|0\rangle\langle 0|(a|0\rangle + b|1\rangle) \\ &= (a^*\langle 0|0\rangle + b^*\langle 1|0\rangle)(a\langle 0|0\rangle + b\langle 0|1\rangle) \\ &= a^*a = |a|^2 \end{aligned} \tag{1.11}$$

The state post-measurement is

$$\frac{M_0|\psi\rangle}{|a|} = \frac{a}{|a|}|0\rangle \tag{1.12}$$

It is only possible to distinguish states if these are orthonormal. If they are not, the measurement will yield a mixture of several states and there can be no reliable procedure to discriminate between them.

Projective Measurement

A projective measurement is described by an observable M, defined as

$$\mathbf{M} = \sum_m m P_m \tag{1.13}$$

where the possible outcomes of the measurement correspond to the eigenvalues m of the observable and P_m is a *projector*, a Hermitian operator.

1.2.2 Entanglement

In the quantum computation context, it is possible to describe composite quantum systems, such as those formed by more than one qubit, by using the tensor product on component systems:

$$|\psi\rangle = \alpha|0\rangle + \beta|1\rangle \tag{1.14}$$
$$|\theta\rangle = \gamma|0\rangle + \delta|1\rangle \tag{1.15}$$
$$|\psi\rangle \otimes |\theta\rangle = \alpha\gamma|00\rangle + \alpha\delta|01\rangle + \beta\gamma|10\rangle + \beta\delta|11\rangle \tag{1.16}$$

Some composites systems, such as

$$|\psi\rangle = \frac{|00\rangle + |11\rangle}{\sqrt{2}} \tag{1.17}$$

cannot be written as a product of states of its component systems. That is, there exists no pair of qubits $\mathsf{Q_a}\rangle = a|0\rangle + b|1\rangle$ and $|\mathsf{Q_b}\rangle = c|0\rangle + d|1\rangle$ that can be combined to form said states.

For the case of two-qubit systems, these special states are called *Bell States*:

$$\mathrm{B}_{00} = \frac{|00\rangle + |11\rangle}{\sqrt{2}} \tag{1.18}$$
$$\mathrm{B}_{01} = \frac{|00\rangle - |11\rangle}{\sqrt{2}} \tag{1.19}$$
$$\mathrm{B}_{10} = \frac{|01\rangle + |10\rangle}{\sqrt{2}} \tag{1.20}$$
$$\mathrm{B}_{11} = \frac{|01\rangle - |10\rangle}{\sqrt{2}}. \tag{1.21}$$

On the other hand, it is possible to *transform* a separable state into a Bell State by applying local operators.

When measuring any qubit from a Bell state, it is possible to immediately know the state of the other qubit. It could be stated that the second qubit measuremente result can be known *a priori*, or that both qubits are communicated through a non-classical correlation.

For example, when measuring the first qubit of the state B_{00}, the states $|0\rangle$ and $|1\rangle$ can be obtained with equal probability $1/2$. If, after measuring, the state $|0\rangle$ is obtained, we already know that the global state has collapsed to $|00\rangle$ and therefore the state of the second qubit is known without performing the corresponding measurement.

This special correlation is called *Entanglement*. This resource cannot be accounted for in classical terms, and is the subject of ongoing research in order to understand it and take advantage of its potential.

1.2.3 Quantum Cryptography

Assymetric cryptography or *public key cryptography* is a scheme used to cipher information. In it, two keys are generated: one used to encrypt the message's information and which can be made public. This is so because the public key is hard to compromise by nature. Another key is used to decode the message. Suppose that Alice and Bob try to communicate. Bob generates a pair of keys, and sends Alice the public key, keeping the other to himself. Alice can use the public key to cypher a message which only Bob can read. A widely employed assymetric or public-key cryptography scheme is the RSA Algorithm (after Rivest, Shamir and Adleman), whose strength is based on the problem of finding the prime factors of a very large integer. No polynomial-time method for factoring large integers on a classical computer has been found yet, although it has not been proven that none exists. The RSA algorithm is used in several day-to-day activities such as e-commerce, and even a computer virus uses it in order to encrypt the victim's data, for whose decrypt key the author asks for a fee (an activity dubbed "ramsomware").

Most notably, quantum computation gained widespread attention when, in 1994, Peter Shor showed [7] that the problem of finding the prime factors in an integer number could be solved *efficiently* –that is, in polynomial time– using a quantum algorithm. Suddenly, one of the most utilized cryptography algorithms turned out to be jeopardized by these new theories.

There exists another kind of cryptography method called symmetrical cryptography or secret-key cryptography, in which said key can be used to cipher the message as well as to decode it. The problem being, obviously, how to ensure a safe delivery of the key.

Recently, a discipline called quantum cryptography has emerged which

makes use of the fact that observation disturbs quantum systems in order to base its reliance. Thusly, it is possible to build a quantum channel for safe key distribution (*Quantum Key Distribution*). Already, commercial solutions exist, and recently, the SECOQC project (founded by the European community through the FP6) demonstrated in October of 2008 a fully functional Quantum Key Distribution network based in Vienna. Remarkably, this form of cryptography makes use of entanglement [5].

1.2.4 Quantum Algorithms

Quantum computers posses the remarkable characteristic that they obey particular laws of probability. The amplitudes of qubits –which relate to the probability of obtaining a particular state after measurement– can be manipulated in such a way that destructive interference cancels out the undesired states, leaving the states of interest with a high probability of measurement.

Grover's algorithm

A class of quantum algorithms is represented by Lov Grover's search algorithm [4]. In this scheme, there is an unsorted database containing $N = 2^n$ items out of which only one meets a given condition. The nature of the condition is such that exact information about it is unknown, preventing the algorithm to directly find a solution, but instead any given item can be tested for the conditions quickly. There is no sorting of the database that could aid its selection. A classical algorithm would examine the different items one by one and would take an average of $N/2$ steps.

Grover's algorithm takes on the order of $\sqrt{N}$ steps to find the desired item. It does so by amplificating the amplitude of the target item.

The algorithm could be used, theoretically, to crack the *Data Encryption Standard*, an algorithm for performing encryption/decryption based on a symmetric-key which enjoyed certain popularity in the 1970's but has since considered insecure for many applications.

Shor's algorithm

Shor's algorithm for factoring integers into their primer components attracted widespread attention towards Quantum Computation and has been since a powerful motivator for the design and building of quantum computers. It is exponentially faster that the fastest classical known factoring algorithm (the *general number field sieve*. It has also inspired a new field

of research ("post-quantum cryptography") which attempts to find better alternatives to the RSA algorithm that are resilient to both quantum and classical computers' attacks.

The algorithm as the following considerations:

- The number to factorise is N.
- A random number x is chosen.
- x is raised to consecutive powers

It turns out that dividing the resulting number by N gives a repeating sequence. The period of the sequence is a factor of the product $(p-1)(q-1)$, with p and q prime factors of N. This means that obtaining periods for different values of x would effectively bring us closer to finding p and q.

Eventhough analyzing the sequence would eventually reveal the period, the number of steps before it repeats could be almost as large as N, which might have hundreds or thousands of digits.

On the other hand, by operating over the enormous quantum superposition of all the numbers of the sequence, it is possible to derive the period because it is a global property of the system, which can be evolved with the quantum equivalent of a Fourier transform.

1.3 Entanglement

1.3.1 How to measure entanglement

By definition, Bell states exemplify the maximum entanglement possible. Is the case of systems comprised by several qubits, there exists various measurements which estimate the amount of entanglement present in the system. Any measurement of entanglement is a non-negative function on a quantum state that cannot increase its entanglement by means of local operations, additionally, it is zero for totally separable states.

One commonly used measurement is the so-called *Entropy of Entanglement*, where the quantum state of the system is considered to be writable as the composite state from subsystems A and B, that is, $|\Psi\rangle = \sum_n \alpha_n |\psi^{\mathsf{A}}\rangle \otimes |\psi^{\mathsf{B}}\rangle$. Using the von Neumann formulation, the entanglement **E** of a pure system is defined as the von Neumann entropy of one of the subsystems A and B,

$$E(|\Psi\rangle) = -\mathrm{tr}(\rho_{\mathsf{A}} \log_2 \rho_{\mathsf{A}}) = -\mathrm{tr}(\rho_{\mathsf{B}} \log_2 \rho_{\mathsf{B}}), \tag{1.22}$$

with tr the *trace* matrix operation and ρ_{A} and ρ_{B} defined as the density matrix of systems A y B, respectively.

In the present work, an alternative method first proposed by Wootters [9] called concurrence, another measurement of entanglement between two qubits in a given quantum system. Concurrence can be calculated using the formula:

$$C(\rho_{\mathsf{A}}) = \max\{0, \lambda_1 - \lambda_2 - \lambda_3 - \lambda_4\}, \tag{1.23}$$

where the coefficients λ_n are the square roots of the eigenvalues of the non-hermitic matrix $\rho_{\mathsf{A}}\tilde{\rho}_{\mathsf{A}}$ in descending order. As with the von Neumann entropy, ρ_{A} is the density matrix of the subsystem formed by the two qubits of interest and is therefore necessary to isolate it from the rest of the system (i.e. the subsystem B. See Fig. 1.2): $\rho_{\mathsf{A}} = \mathrm{tr}_{\mathsf{B}}(\rho)$.

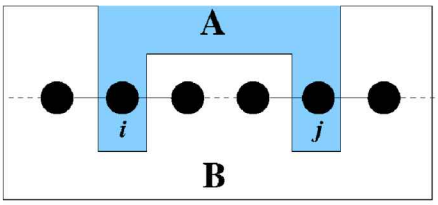

Figure 1.2: The system is divided into two subsystems for the calculation of Concurrence between qubits i and j.

Matrix $\tilde{\rho}$ is obtained making use of the transformation defined as

$$\tilde{\rho_{\mathsf{A}}} = (\sigma_y \otimes \sigma_y)\rho_{\mathsf{A}}^{*}(\sigma_y \otimes \sigma_y) \tag{1.24}$$

with σ_y the Pauly operator $\mathbf{Y}$,

$$\mathbf{Y} \equiv \begin{pmatrix} 0 & -i \\ i & 0 \end{pmatrix} \tag{1.25}$$

Bibliography

[1] Mark T. Bohr, Robert S. Chau, Tahir Ghani, and Kaizad Mistry. The high-k solution. `http://spectrum.ieee.org/semiconductors/design/the-highk-solution`, October 2007.

[2] David Deutsch. Quantum theory, the church-turing principle and the universal quantum computer. *Proceedings of the Royal Society of London A*, 400:97–117, 1985.

[3] Richard P. Feynman. Simulating physics with computers. *International Journal of Theoretical Physics*, 21(6), 1982.

[4] Lov K. Grover. A fast quantum mechanical algorithm for database search. *Annual ACM Symposium on the Theory of Computing (STOC)*, pages 212–219, 1996.

[5] H. Hübel, M. R. Vanner, T. Lederer, B. Blauensteiner, T. Lorünser, A. Poppe, and A. Zeilinger. High-fidelity transmission of polarization encoded qubits from an entangled source over 100 km of fiber. *Optics Express*, 15:7853–7862, 2007.

[6] Claude Elwood Shannon. A symbolic analysis of relay and switching circuits. Master's thesis, Massachusetts Institute of Technology, Dept. of Electrical Engineering, 1940.

[7] P. W. Shor. Algorithms for quantum computation: Discrete logarithms and factoring. *Proceedings, 35th Annual Symposium on Foundations of Computer Science*, pages 124–134, 1994.

[8] Robert Solovay and Volker Strassen. A fast monte-carlo test for primality. *SCIAM Journal of Computing*, 6(1):84–85, 1977.

[9] William K. Wootters. Entanglement of formation of an arbitrary state of two qubits. *Physical Review Letters*, 80(10):2245–2248, 1992.

Chapter 2

Maximizing Entanglement

Our efforts have focused on the maximization of Entanglement in different periodical systems through the measurement known as Concurrence.

These ideas of optimization are rooted in the work of O'Connor and Wootters [4] where a maximum in Concurrence is found between first neighbors in translationally invariant chains. Two restrictions are imposed on the wave-function over which the process of optimization is carried on. Specifically, it is required that the $|\Psi\rangle$ state of the chain be an eigenstate of the total spin component, and that the neighbor particles cannot have the same $|\uparrow\rangle$ state.

Working with these restrictions, O'Connor and Wootters show that the concurrence can be written as

$$C = \frac{N-p}{N} C' \tag{2.1}$$

where C' is defined as a pseudo-Concurrence,

$$C' = -\left(\frac{1}{N-p}\right) \langle\phi|H|\phi\rangle, \tag{2.2}$$

N is the number of sites and p is the number of particles with spin up. $\hat{H}$ is the operator defined as

$$\hat{H} = -\sum_{j=1}^{N-p} (a_j^\dagger a_{j+1} + a_{j+1}^\dagger a_j) \tag{2.3}$$

with $a_j^\dagger$ (a_j) a creation (destruction) operator. This means that a $|\phi\rangle$ state maximizes C if it minimizes the spectation value of the $\hat{H}$ operator, which is a Hamiltonian for the XY ferromagnetic, one-dimensional model with $N-p$ sites. This optimization problem can be therefore solved by finding the

lowest energy level. The solution of the problem begins by noting that the operators $a^\dagger$ and a are not fermionic operators because $[a_j^\dagger, a_k^\dagger] = [a_j^\dagger, a_k] = [a_j, a_k] = 0$ when $j \neq k$ while true fermionic operators anti-commute. That is why it is necessary to define true fermionic operators $c^\dagger$ and c through the Jordan-Wigner transform

$$c_j = \exp\left[i\pi \sum_{k=1}^{j-1} a_k^\dagger a_k\right] a_j$$
$$c_j^\dagger = a_j^\dagger \exp\left[-i\pi \sum_{k=1}^{j-1} a_k^\dagger a_k\right].$$

In terms of these operators, $\hat{H}$ can be written as

$$\hat{H} = -\sum_{j=1}^{N-p} \left(c_j^\dagger c_{j+1} + c_{j+1}^\dagger c_j\right) \tag{2.4}$$

for odd p, and

$$\hat{H} = -\sum_{j=1}^{N-p-1} \left(c_j^\dagger c_{j+1} + c_{j+1}^\dagger c_j\right) + \left(c_{N-p}^\dagger c_1 + c_1^\dagger c_{N-p}\right) \tag{2.5}$$

when p even.

Note that this is a tight-binding Hamiltonian for a system with $N - p$ sites with hopping integral $t_{ij} = -1$ between first neighbors.

2.1 Genetic Algorithms

As optimization method, we employed the genetic algorithm (GA) technique, first developed by John Henry Holland and his students in the University of Michigan in the 1960's and 70's. Holland's goal was not to develop an algorithm for a specific problem, but rather to formally study the phenomena of adaptation as it happens in nature and mimick the different processes involved in order to apply them into a general-purpose optimization algorith.

In this technique, a set of characters that represent a potential solution to the problem are stored in a chain called "chromosome". The *encoding* of the solution is often a crucial step in the success of the algorithm. The final encoding depends strongly on the problem, and can involve fixed

or variable chromosome length, and could work with regular real-valued numbers, or directly at binary level.

The algorithm starts creating a collection of such chromosomes ("population"). Crossover and mutation operators, inspired in nature, are applied on the population's individuals in order to create new chromosomes. In the present work, two varians of the crossover operator were used: each pair of chromosomes where crossed either at a randomly chosen single point, or two points, equally spaced.

Each individual is subsequently tested with an evaluating function which assigns them a score (the *fitness* function). Depending on the goal of the problem, the evaluating function can effectively lead the algorithm to minimizing or maximizing a certain quantity, or could tune a combination of several outputs (in which case the research is focused rather on the *form* of the answer)

A new population is formed by choosing individuals with a probability dependent of their score. The *selection method* can be enhanced with some kind of scaling for preventing early high-scoring individuals to saturate the population early on and drive the solutions to a confined portion of the solution space. To address such issue, we have employed Sigma Scaling [2]:

$$\text{Expected value } = \begin{cases} 1 + \frac{f(i) - \langle f(t) \rangle}{2\sigma} & \text{if } \sigma(t) \neq 0 \\ 1.0 & \text{if } \sigma(t) = 0 \end{cases} \tag{2.6}$$

with $f(i)$ being the individual's current scored fitness, $\langle f(t) \rangle$ the population's average fitness at time (generation) t, and σ being the standard deviation of the population's fitness, $\sqrt{\langle f^2(t) \rangle - \langle f(t) \rangle^2}$. At the beginning of a run, when the standard deviation of fitnesses is typically high, the fittest individuals are to be scaled down, preventing them to overrrun the next population. Later in the run, when the population is typically more converged and the standard deviation is lower, the fittest individuals will stand out more.

The process is repeated until a terminating condition is met. Usually running time, desired fitness, relative change between generations and number of generations are the most common. In this work we have employed the latter.

Using this approach, it is possible to obtain a good solution without having to explore the entire solution-space, which, depending on the problem, could be impractical. On the other hand, the efficiency or the process depends greatly on several variables: the crossover and mutation probability, the number of generations, the population size and the selection criterion.

Although, in general, genetic algorithms allow the finding of very good solutions with ease, the process is, depending on the problem, subject to get stuck in local minima (or maxima) without possibility of exploring other regions of the solution-space.

2.2 Our model

The system on which we have performed our simulations is a periodic network modelled with a Tight-Binding Hamiltonian, that is, a Hamiltonian similar to the one in Eq. 2.4. The main difference is that, for our case, it goes to the N site, and the hopping integrals t_{ij} will be optimized. The Tight-Binding Hamiltonian in our work is

$$\hat{H} = \sum_i \varepsilon_i \hat{n}_i + \sum_{\langle ij \rangle} t_{ij} \hat{c}_i^\dagger \hat{c}_j \tag{2.7}$$

where, for simplicity, we work with the same kind of atoms and take $\varepsilon_i = 0$. Spinless electrons are also considered.

The state $|0\rangle$ is modelled by an empty site, and the state $|1\rangle$ by an electron-occupied site. In each case we vary the number of electrons in the system. For the optimization procedure, the "chromosomes" of the genetic algorithm are nothing more than the hopping elements t_{ij} between sites. The allowed range for their values are $-5 \geq t_{ij} \geq 0$.

2.2.1 The density matrix

In this particular model, in order to obtain an analytic expression for the Concurrence between two qubits, it is necessary to obtain the corresponding density matrix ρ_A of the subsystem comprised of the qubits of interest.

For any particular number N_1 of occupied sites and $N - N_1$ unoccupied sites, the two-qubit subsystem has naturally four possible states, and the general state function describing the system, namely

$$|\psi_{AB}\rangle = \sum_n \alpha_n |\psi_A\rangle |\psi_B\rangle, \tag{2.8}$$

can be separated in the following manner:

$$|\psi_{AB}\rangle = \sum_m \alpha_{00}|00\rangle \otimes |\psi_B^m\rangle + \sum_o \alpha_{01}|01\rangle \otimes |\psi_B^o\rangle + \sum_p \alpha_{10}|10\rangle \otimes |\psi_B^p\rangle + \sum_q \alpha_{11}|11\rangle \otimes |\psi_B^q\rangle. \tag{2.9}$$

The sums over m, o, p and q run over all the possible combinations of the states comprising the rest of the system such that the number of occupied sites is preserved.

To obtain the reduced density matrix is is necessary to perform the trace over subsystem B, that is,

$$\rho_A = \sum_{k=1}^{2^{N-2}} \big(\langle I| \otimes \langle \psi_B^k|\big)|\psi_{AB}\rangle\langle\psi_{AB}|\big(|I\rangle \otimes |\psi_B^k\rangle\big). \tag{2.10}$$

(notice that the summation runs over $N-2$, accounting for the two qubits left out for the subsystem A). As an example, consider the case with $N = 4, N_1 = 1$ and the subsystem A being the two rightmost qubits. The possible states are

$$\alpha_1|0001\rangle + \alpha_2|0010\rangle + \alpha_4|0100\rangle + \alpha_8|1000\rangle \tag{2.11}$$

and the density matrix for the whole system is

$$\begin{aligned}
|\psi_{AB}\rangle\langle\psi_{AB}| = {} & \alpha_1^*\alpha_1|0001\rangle\langle 0001| + \alpha_1^*\alpha_2|0001\rangle\langle 0010| \\
& + \alpha_1^*\alpha_4|0001\rangle\langle 0100| + \alpha_1^*\alpha_8|0001\rangle\langle 1000| \\
& + \alpha_2^*\alpha_1|0010\rangle\langle 0001| + \alpha_2^*\alpha_2|0010\rangle\langle 0010| \\
& + \alpha_2^*\alpha_4|0010\rangle\langle 0100| + \alpha_2^*\alpha_8|0010\rangle\langle 1000| \\
& + \alpha_4^*\alpha_1|0100\rangle\langle 0001| + \alpha_4^*\alpha_2|0100\rangle\langle 0010| \\
& + \alpha_4^*\alpha_4|0100\rangle\langle 0100| + \alpha_4^*\alpha_8|0100\rangle\langle 1000| \\
& + \alpha_8^*\alpha_1|1000\rangle\langle 0001| + \alpha_8^*\alpha_2|1000\rangle\langle 0010| \\
& + \alpha_8^*\alpha_4|1000\rangle\langle 0100| + \alpha_8^*\alpha_8|1000\rangle\langle 1000|
\end{aligned} \tag{2.12}$$

The reduced density matrix operator is thus

$$\begin{aligned}
\rho_A = {} & \langle 00xx|\psi_{AB}\rangle\langle\psi_{AB}|00xx\rangle + \langle 01xx|\psi_{AB}\rangle\langle\psi_{AB}|01xx\rangle \\
& + \langle 10xx|\psi_{AB}\rangle\langle\psi_{AB}|10xx\rangle + \langle 11xx|\psi_{AB}\rangle\langle\psi_{AB}|11xx\rangle
\end{aligned} \tag{2.13}$$

This operation will eliminate by orthogonality all but those states whose elements in the B subsystem have the same number of occupied sites. For example, the first term of ρ_A is:

$$\langle 00xx|\psi_{AB}\rangle\langle\psi_{AB}|00xx\rangle = \alpha_1^*\alpha_1 + \alpha_1^*\alpha_2 + \alpha_2^*\alpha_1 + \alpha_2^*\alpha_2. \tag{2.14}$$

That, in turn, means that also subsystem A has to preserve the number of occupied states, leaving only certain elements in the ρ_A matrix:

$$\rho_A = \begin{pmatrix} \rho_{11} & 0 & 0 & 0 \\ 0 & \rho_{22} & \rho_{23} & 0 \\ 0 & \rho_{32} & \rho_{33} & 0 \\ 0 & 0 & 0 & \rho_{44} \end{pmatrix}. \tag{2.15}$$

For ρ_A to be a valid density matrix, it has to be Hermitic ($\rho_A = \rho_A^{\dagger *}$) and its trace be equal to 1. This means that $\rho_{32} = \rho_{23}^*$ and $\rho_{11}+\rho_{22}+\rho_{33}+\rho_{44} = 1$ so it is necessary to calculate only four elements of the matrix.

2.2.2 The density matrix elements

Each element of the reduced density matrix can be calculated using the second quantization approach.

The first element of the matrix, ρ_{11} can be realized as follows

$$\rho_{11} = \langle\psi_{AB}|\big(1-\hat{n}_i\big)\big(1-\hat{n}_j\big)|\psi_{AB}\rangle \tag{2.16}$$

where the operator $\hat{n}_j$ finds all the elements of the type $|x1\rangle \otimes |\psi_B\rangle$ and after applying $(1-\hat{n}_j)$ we end up with all the elements that do *not* occupy the site j (i.e. $|x0\rangle \otimes |\psi_B\rangle$). A similar approach follows $(1-\hat{n}_i)$ and after applying the bra operation we are left only with the coefficients of all the $|00\rangle \otimes |\psi_B\rangle$ states.

Likely, the other elements are obtained with the following operators:

$$\rho_{22} = \langle\psi_{AB}|\big(1-\hat{n}_i\big)\hat{n}_j|\psi_{AB}\rangle \tag{2.17}$$
$$\rho_{33} = \langle\psi_{AB}|\hat{n}_i\big(1-\hat{n}_j\big)|\psi_{AB}\rangle \tag{2.18}$$
$$\rho_{44} = \langle\psi_{AB}|\hat{n}_i\hat{n}_j|\psi_{AB}\rangle \tag{2.19}$$
$$\rho_{23} = \langle\psi_{AB}|c_j c_i^\dagger|\psi_{AB}\rangle. \tag{2.20}$$

In the last equation, $c_i^\dagger$ leaves only those states with the form $|0x\rangle \otimes |\psi_B\rangle$ and transforms them into $|1x\rangle \otimes |\psi_B\rangle$. Out of this set of states, c_j deletes a particle at site j from all states of the type $|x1\rangle \otimes |\psi_B\rangle$ and we end up with states $|10\rangle \otimes |\psi_B\rangle$.

It is very easy to show that the ρ_A elements can be calculated as average quantities of the complete ground-state wave function. For example,

$$\begin{aligned} \rho_{11} =& \langle\psi_{AB}|\psi_{AB}\rangle - \langle\psi_{AB}|\hat{n}_i|\psi_{AB}\rangle - \langle\psi_{AB}|\hat{n}_j|\psi_{AB}\rangle \\ &+ \langle\psi_{AB}|\hat{n}_i\hat{n}_j|\psi_{AB}\rangle \\ =& 1 - \langle\hat{n}_i\rangle - \langle\hat{n}_j\rangle + \langle\hat{n}_i\hat{n}_j\rangle. \end{aligned} \tag{2.21}$$

The other elements are obtained similarly:

$$\begin{array}{ll} \rho_{22} = \langle \hat{n}_j \rangle - \langle \hat{n}_i \hat{n}_j \rangle & \rho_{33} = \langle \hat{n}_i \rangle - \langle \hat{n}_i \hat{n}_j \rangle \\ \rho_{44} = \langle \hat{n}_i \hat{n}_j \rangle & \rho_{23} = \langle c_j c_i^\dagger \rangle \end{array} \tag{2.22}$$

2.2.3 Concurrence

In order to use the Concurrence formula (1.23), the non-Hermitian matrix $\rho_A \tilde{\rho_A}$ must be calculated. The matrix $\tilde{\rho_A}$ is constructed using (1.24):

$$\tilde{\rho_a} = \begin{pmatrix} 0 & 0 & 0 & -1 \\ 0 & 0 & 1 & 0 \\ 0 & 1 & 0 & 0 \\ -1 & 0 & 0 & 0 \end{pmatrix} \begin{pmatrix} \rho_{11}^* & 0 & 0 & 0 \\ 0 & \rho_{22}^* & \rho_{23}^* & 0 \\ 0 & \rho_{32}^* & \rho_{33}^* & 0 \\ 0 & 0 & 0 & \rho_{44}^* \end{pmatrix} \begin{pmatrix} 0 & 0 & 0 & -1 \\ 0 & 0 & 1 & 0 \\ 0 & 1 & 0 & 0 \\ -1 & 0 & 0 & 0 \end{pmatrix} \tag{2.23}$$

$$= \begin{pmatrix} 0 & 0 & 0 & -\rho_{44}^* \\ 0 & \rho_{32}^* & \rho_{33}^* & 0 \\ 0 & \rho_{22}^* & \rho_{23}^* & 0 \\ -\rho_{11}^* & 0 & 0 & 0 \end{pmatrix} \begin{pmatrix} 0 & 0 & 0 & -1 \\ 0 & 0 & 1 & 0 \\ 0 & 1 & 0 & 0 \\ -1 & 0 & 0 & 0 \end{pmatrix} \tag{2.24}$$

$$= \begin{pmatrix} \rho_{44}^* & 0 & 0 & 0 \\ 0 & \rho_{33}^* & \rho_{32}^* & 0 \\ 0 & \rho_{23}^* & \rho_{22}^* & 0 \\ 0 & 0 & 0 & \rho_{11}^* \end{pmatrix} \tag{2.25}$$

Now we are able to construct the non-Hermitian matrix $\rho_A \tilde{\rho_A}$:

$$\rho_A \tilde{\rho_A} = \begin{pmatrix} \rho_{11} & 0 & 0 & 0 \\ 0 & \rho_{22} & \rho_{23} & 0 \\ 0 & \rho_{32} & \rho_{33} & 0 \\ 0 & 0 & 0 & \rho_{44} \end{pmatrix} \begin{pmatrix} \rho_{44}^* & 0 & 0 & 0 \\ 0 & \rho_{33}^* & \rho_{32}^* & 0 \\ 0 & \rho_{23}^* & \rho_{22}^* & 0 \\ 0 & 0 & 0 & \rho_{11}^* \end{pmatrix} \tag{2.26}$$

$$= \begin{pmatrix} \rho_{11}\rho_{44}^* & 0 & 0 & 0 \\ 0 & \rho_{22}\rho_{33}^* + \rho_{23}\rho_{23}^* & \rho_{22}\rho_{32}^* + \rho_{23}\rho_{22}^* & 0 \\ 0 & \rho_{32}\rho_{33}^* + \rho_{33}\rho_{23}^* & \rho_{32}\rho_{32}^* + \rho_{33}\rho_{22}^* & 0 \\ 0 & 0 & 0 & \rho_{11}^*\rho_{44} \end{pmatrix} \tag{2.27}$$

but ρ_A is indeed Hermitian so the following relationships are taken into account: $\rho_{11} = \rho_{11}^*$, $\rho_{22} = \rho_{22}^*$, $\rho_{32} = \rho_{23}^*$, $\rho_{33} = \rho_{33}^*$ y $\rho_{44} = \rho_{44}^*$. The matrix

$\rho_A\tilde{\rho_A}$ now has the form

$$\rho_A\tilde{\rho_A} = \begin{pmatrix} \rho_{11}\rho_{44} & 0 & 0 & 0 \\ 0 & \rho_{22}\rho_{33} + \rho_{23}\rho_{23}^* & \rho_{22}\rho_{23} + \rho_{23}\rho_{22} & 0 \\ 0 & \rho_{23}^*\rho_{33} + \rho_{33}\rho_{23}^* & \rho_{22}\rho_{33} + \rho_{23}\rho_{23}^* & 0 \\ 0 & 0 & 0 & \rho_{11}\rho_{44} \end{pmatrix} \tag{2.28}$$

$$= \begin{pmatrix} \rho_{11}\rho_{44} & 0 & 0 & 0 \\ 0 & \rho_{22}\rho_{33} + \rho_{23}\rho_{23}^* & 2\rho_{22}\rho_{23} & 0 \\ 0 & 2\rho_{33}\rho_{23}^* & \rho_{22}\rho_{33} + \rho_{23}\rho_{23}^* & 0 \\ 0 & 0 & 0 & \rho_{11}\rho_{44} \end{pmatrix} \tag{2.29}$$

$$= \begin{pmatrix} \rho_{11}\rho_{44} & 0 & 0 & 0 \\ 0 & \rho_{22}\rho_{33} + |\rho_{23}|^2 & 2\rho_{22}\rho_{23} & 0 \\ 0 & 2\rho_{33}\rho_{23}^* & \rho_{22}\rho_{33} + |\rho_{23}|^2 & 0 \\ 0 & 0 & 0 & \rho_{11}\rho_{44} \end{pmatrix}. \tag{2.30}$$

In a block diagonal matrix, eigenvalues are simply the eigenvalues of individual blocks so two eigenvalues are readily available. The other two are obtained calculating the determinant of:

$$\begin{pmatrix} \rho_{22}\rho_{33} + |\rho_{23}|^2 - \lambda & 2\rho_{22}\rho_{23} \\ 2\rho_{33}\rho_{23}^* & \rho_{22}\rho_{33} + |\rho_{23}|^2 - \lambda \end{pmatrix}. \tag{2.31}$$

which simply is

$$(\rho_{22}\rho_{33} + |\rho_{23}|^2 - \lambda)^2 - 4\rho_{22}\rho_{33}|\rho_{23}|^2 = 0. \tag{2.32}$$

And now we simply find the value of λ

$$(\rho_{22}\rho_{33} + |\rho_{23}|^2 - \lambda)^2 = 4\rho_{22}\rho_{33}|\rho_{23}|^2 \tag{2.33}$$

$$\rho_{22}\rho_{33} + |\rho_{23}|^2 - \lambda = \pm 2\sqrt{\rho_{22}\rho_{33}}|\rho_{23}| \tag{2.34}$$

$$\lambda = \rho_{22}\rho_{33} + |\rho_{23}|^2 \mp 2\sqrt{\rho_{22}\rho_{33}}|\rho_{23}| \tag{2.35}$$

which yields the values for the λ coefficients:

$$\lambda_a = \rho_{22}\rho_{33} - 2\sqrt{\rho_{22}\rho_{33}}|\rho_{23}| + |\rho_{23}|^2 = (\sqrt{\rho_{22}\rho_{33}} - |\rho_{23}|)^2 \tag{2.36}$$

$$\lambda_b = \rho_{22}\rho_{33} + 2\sqrt{\rho_{22}\rho_{33}}|\rho_{23}| + |\rho_{23}|^2 = (\sqrt{\rho_{22}\rho_{33}} + |\rho_{23}|)^2 \tag{2.37}$$

$$\lambda_c = \rho_{11}\rho_{44} \tag{2.38}$$

$$\lambda_d = \rho_{11}\rho_{44}. \tag{2.39}$$

Finally, to be able to use equation (1.23) we use the square roots of the

lambda coefficients:

$$\sqrt{\lambda_a} = \sqrt{\rho_{22}\rho_{33}} - |\rho_{23}| \tag{2.40}$$
$$\sqrt{\lambda_b} = \sqrt{\rho_{22}\rho_{33}} + |\rho_{23}| \tag{2.41}$$
$$\sqrt{\lambda_c} = \sqrt{\rho_{11}\rho_{44}} \tag{2.42}$$
$$\sqrt{\lambda_d} = \sqrt{\rho_{11}\rho_{44}} \tag{2.43}$$

Notice that λ_b is the largest eigenvalue. The final formula becomes

$$C = \max\{0, \sqrt{\rho_{22}\rho_{33}} + |\rho_{23}| - \sqrt{\rho_{22}\rho_{33}} + |\rho_{23}| - \sqrt{\rho_{11}\rho_{44}} - \sqrt{\rho_{11}\rho_{44}}\} \tag{2.44}$$
$$C = \max\{0, 2|\rho_{23}| - 2\sqrt{\rho_{11}\rho_{44}}\} \tag{2.45}$$
$$C = 2\max\{0, |\rho_{23}| - \sqrt{\rho_{11}\rho_{44}}\} \tag{2.46}$$

Thus, for this particular model, it is possible to obtain an analytic expression for the Concurrence:

$$C = 2\max\{0, |\rho_{23}| - \sqrt{\rho_{11}\rho_{44}}\} \tag{2.47}$$

with

$$\begin{aligned} \rho_{23} &= \langle c_j c_i^\dagger \rangle, \\ \rho_{11} &= 1 - \langle \hat{n}_i \rangle - \langle \hat{n}_j \rangle + \langle \hat{n}_i \hat{n}_j \rangle \\ \rho_{44} &= \langle \hat{n}_i \hat{n}_j \rangle \end{aligned} \tag{2.48}$$

2.3 First results

We previously employed genetic algorithms in order to optimize the total Concurrence C_{total} in 1-dimensional and 2-dimensional lattices described by a Tight-Binding Hamiltonian with periodic and open boundary conditions. C_{total} was calculated as the average Concurrence between each site i with the remaining $N-1$. This is

$$C_{total} = \frac{1}{N(N-1)} \sum_{i=1}^{N} \sum_{j \neq i}^{N} C_{ij}. \tag{2.49}$$

Our numerical results ([3]) show a accordance with the theorethical formula proposed by Koashi *et al.* [1] (see Fig. 2.1), who give an upper limit to Concurrence of $2/N$ for this setup, which is when only one qubit is found in the state $|1\rangle$ ($|0\rangle$) and the other $N-1$ qubits are in the state $|0\rangle$ ($|1\rangle$). In our case, this corresponds to the start and end of electron-filling.

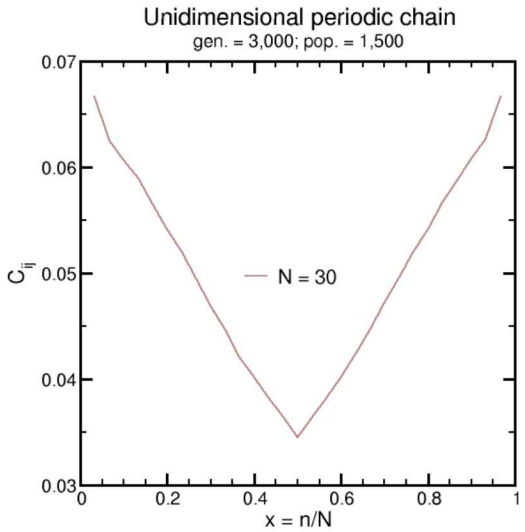

Figure 2.1: Concurrence between all sites for a 1-dimensional periodic lattice as function of electronic filling. Koashi *et al.* show an upper limit of $2/N$ for this case

Bibliography

[1] Masato Koashi, Vladimír Buzek, and Nobuyuki Imoto. Entangled webs: Tight bound for symmetric sharing of entanglement. *Physical Review A*, 62(050302(R)):1–4, 2000.

[2] Melanie Mitchell. *An Introduction to Genetic Algorithms*. MIT Press, Cambridge, MA, USA, 1998.

[3] J. C. Navarro-Muñoz, H. C. Rosu, and R. López-Sandoval. Genetic algorithm optimization of entanglement. *Physical Review A*, 74(052308):1–8, 2006.

[4] Kevin M. O'Connor and William K. Wotters. Entangled rings. *Physical Review A*, A(052302):1–9, 2001.

Chapter 3

Designing lattice structures with maximal nearest neighbor Concurrence

The ideas of optimization can be further explored in two manners.

On one hand, it is known that two qubits fully entangled cannot entangle with a third qubit. This property is known as monogamy [1], and imposes restrictions over quantum correlations. How does monogamy affects maximum entanglement on a number of N qubits?

On the other hand, Quantum Phase Transitions (QPTs) occur at zero temperature. It is common that several kinds of interactions exist near a quantum critical point between phases, so little changes in control parameters (e.g. pressure, stress in a particular direction, chemical substitution, magnetic field etc.) can favor one kind over the others. These fluctuations are quantum in nature, and have great influence in the phase diagram, compared with thermal fluctuations.

The existance of these kinds of exotic states is hard to predict. Due to the difficulty to solve a few-particle system exactly, it is impossible to deal with a life-like problem using a first principles approach.

Our studies on Concurrence can be an interesting tool that can help to understand the relationship between the wave functions corresponding to a maximum in average Concurrence and Quantum Phase Transitions. For example, Gu *et al*. [3] found that the behavior of Entanglement for a chain modelled after an extended Hubbard Hamiltonian is related with the quantum phase diagram of such system.

We have, therefore, focused on first neighbor Concurrence:

$$C_{\mathrm{NN}} = \frac{1}{zN} \sum_{i=1}^{N} \sum_{j}^{z} C_{ij}, \tag{3.1}$$

where z is the number of first neighbors.

Note that, in contrast with our case, a system with translational invariance is equivalent to having all the t_{ij} elements of the Hamiltonian 2.7 with the same value, for example $t_{ij} = -1$. That particular configuration yields the same value of Concurrence for each pair of neighbors [5, 8].

In order to tune each t_{ij} element in our system, we employ the following pseudo-algorithm:

1. We consider each t_{ij} element from the Hamiltonian matrix as a gene, and the array of all genes that correspond to a pair of first neighbors as a *chromosome*.

2. Space in memory is reserved for arrays of chromosomes: "$\mathrm{generation0}$" and "$\mathrm{generation1}$".

3. Memory space is reserved for a "best" chromosome with fitness value 0.0.

4. For a given band filling $x = n/N$ (with N the total number of sites and n the number of electrons in the system), repeat

    - Initialize $\mathrm{generation0}$. Each of its chromosomes' values are set to a random number in the range $(-5, 0)$.
    - For a number of generations, repeat
        - Each chromosome in $\mathrm{generation0}$ is decoded into a Hamiltonian matrix, which is diagonalized. The average Concurrence between first neighbors is calculated using Eq. 3.1. C_{NN} becomes, thusly, the value of fitness for each individual in $\mathrm{generation0}$.
        - Compare each individual in $\mathrm{generation0}$ with the chromosome best. If the former's fitness value is greater than the latter, substitute.
        - Choose chromosomes with a probability proportional to their fitness, and copy them to $\mathrm{generation1}$.
        - Crossover and mutation operators are applied on each individual of $\mathrm{generation1}$ with certain probability (0.6 and 0.02, respectively).

- $\mathrm{generation1}$ becomes $\mathrm{generation0}$.

- Print best in an output file.

At the end of the run, the program yields the best average value of Concurrence found, as well as the corresponding configuration for each electron number.

Said configuration is a vector made from all the non-zero elements of the hopping elements from the Hamiltonian matrix packed in columns.

In the following sections, we present our results of nearest-neighbor Concurrence optimization using genetic algorithms. The effect of bipartite and non-bipartite systems with periodic boundary conditions is addressed. Biparticity or non-biparticity has important consequeneces in the physical properties of a lattice. For example, the Concurrence of a bipartite lattice is symmetric around half band filling while non-biparticity is responsible for magnetic frustration in spin systems, that is, the impossibility of minimizing energy for each pair of spins in the lattice.

3.0.1 One dimensional lattice

The first case analyzed was the one dimensional chain with periodical boundary conditions. It is a bipartite lattice, a property related with the symmetry of the system. A bipartite lattice is such that can be separated into two sub-lattices in such way that each neighbor from the first lattice belongs to the the second, and the other way around.

In the case of the ring, the behavior of average Concurrence (from now on, understood as limited between first neighbors) can be seen in Figure 3.1. The "ordered" case, with all elements $t_{ij} = -1.0$ is also shown in the figure. The optimized system was comprised of 50 sites, and the algorithm was run with 4000 generations and a population size of 500.

From the figure, it can immediately be seen that there is symmetry around half filling which is due to its biparticity. It is also possible to observe that the optimized case is capable of finding a much better solution. In both cases, there is only one maximum.

After noticing a pattern in the values of the t_{ij} elements found in the best chromosome, we wrote a program to visually inspect it. Figure 3.2 shows the one dimensional chain.

The visualizing tool shows strong values ($|t_{ij}| \geq 3$) in black, relatively weak values ($3 > |t_{ij}| \geq 1$) in dark-gray and weak values ($1 > |t_{ij}| \geq 0$) in light-gray. Note how strong hopping elements alternate with weak ones. This indicates that the conditions imposed by the algorithm (i.e. finding a high average Concurrence between first neighbors) pushed the system

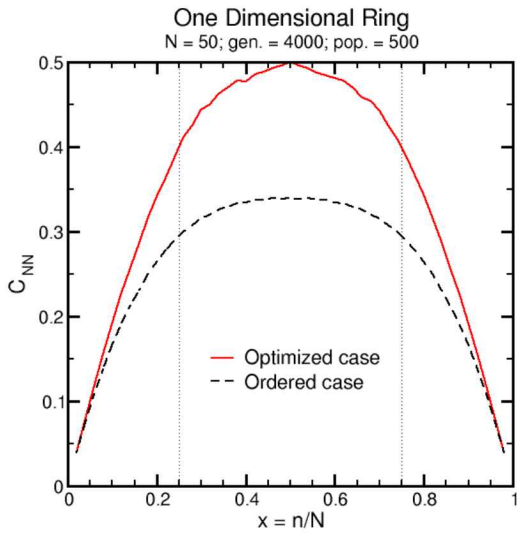

Figure 3.1: Average Concurrence between first neighbors for a periodic one dimensional lattice as a function of electronic filling. The ordered and optimized case are shown.

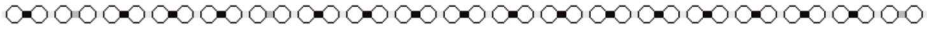

Figure 3.2: One dimensional chain at half electronic filling. This particular configuration corresponds to the maximum shown in Fig. 3.1

into a Peierls-like transition with alternating interaction values. This is a metal-insulator transition occurring in one-dimensional metals, where the doubling of the unit cell leads to a decrease in the kinetic energy of the system.

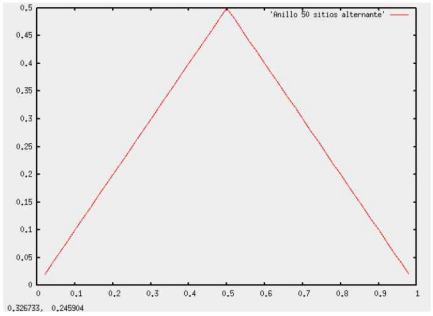

Figure 3.3: Average Concurrence for a ring with alternating values of interaction.

To explain this behavior, we can analyze a subsystem of three qubits where the middle qubit is labeld b. This site has a strong interaction with one if its neighbor, say, c, but a very weak one with the other, a. This means that, at half filling —when there is one electron for each pair of sites—, site b is sharing an electron with site c whereas is sharing none with site a. We modelled our system with a $|0\rangle$ state represented by an empty site and a

$|1\rangle$ state by an occupied one, so the subsystem $a-b$ is in the state $|00\rangle$. On the other hand, the subsystem $b-c$ has one electron, but it is unknown which site is occupying. This means that the $b-c$ subsystem is in the state $|01\rangle+|10\rangle$ –one of the Bell States. By definition, each Bell State has a Concurrence of 1 (i.e. maximum inseparability) whereas the $|00\rangle$ can be separated completely and has a Concurrence of 0. When taking the average between the two, the average is simply 0.5. This is repeated for a many-sites system. This explains why the maximum is found at half filling and corresponds to a configuration as the one in Fig. 3.2.

It is important to note that the weak interactions are only close to zero, but the ring has not fully broken into isolated subsystems. This is important as completely dimerized chains consisting of isolated dimers would show highly localized entanglement, which cannot be fully exploited as a system property. Fortunately, it is not necessary to reach the fully dimerized lattice in order to achieve high entanglement, as can be seeen in Figure 3.4, where the nearest-neighbor Concurrence almost saturates to the maximal value when the ratio between successive hopping elements becomes equal to 10, which means that the system is far from being fully dimerized but exhibits almost the maximal entanglement.

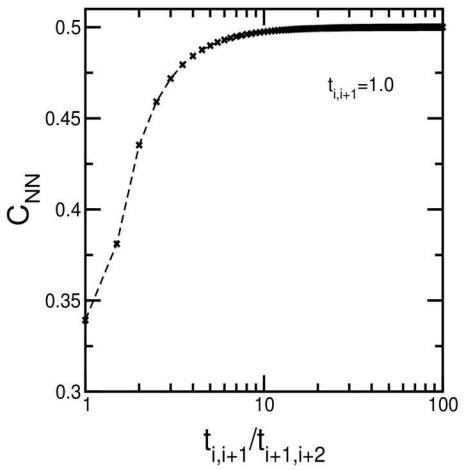

Figure 3.4: Nearest neighbor Concurrence of a tight-binding dimerized chain as a function of its dimerization $t_{i,i+1}/t_{i+1,i+2}$ with $t_{i,i+1}=1.0$.

We also calculate the average Concurrence fixing the hopping values for this particular alternating setup, for each filling. In contrast with the optimized case which presented a quasi-parabolic curve, the alternating setup is completely linear (see Figure 3.3).

This behavior can be explained if we remember that each electron added to the system represents an additional $|11\rangle$ state, which decreases the average Concurrence. The same occurs if we move to the left of Fig.

3.3, as we are adding $|00\rangle$ states to the setup. Each electron added or taken represents an added 0 to the average Concurrence, hence the linear behavior.

3.0.2 Square lattice

Now we analyze the simplest two-dimensional case: the square lattice. The sites in this kind of lattices have four first neighbors. The behavior of Concurrence under the optimization procedure can be seen in Figure 3.5. The lattice size was 36 sites and the algorithm was run with 10000 generations and 700 individuals.

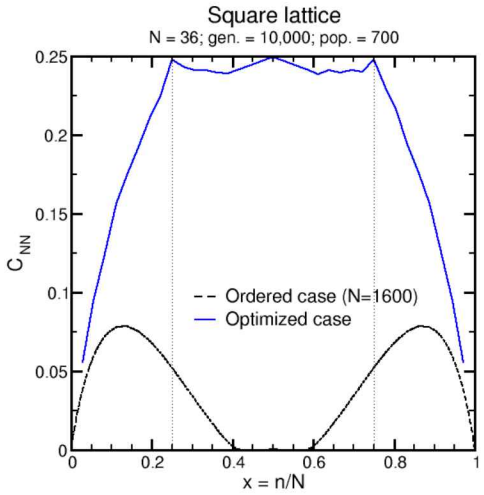

Figure 3.5: Average Concurrence for a square lattice. Ordered and optimized case.

There are several noteworthy facts. Once again, it is possible to note that the optimization algorithm yields a better curve than the ordered case. Secondly, this curve has three maxima, each peaking at an average Concurrence of 0.25. It is also important to mention that there is symmetry around half filling, due to the square lattice also being a bipartite lattice.

What happens when we study the chromosomes corresponding to the maxima? We employed our visualization tool has in the case of the one dimensional lattice. Results are shown in Figure 3.6.

As in the one dimensional chain, it is possible to identify certain patterns or special configurations in the system. In the case $x = 0.25$, for example, the system tries to form electronic islands, while the case 0.5 is more similar to the one dimensional case: As each site shares one electron with one of its four neighbors (Bell state B_{00}, $C = 1$) and none with the

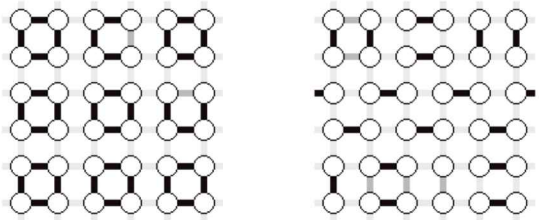

(a) Filling $x = 0.25$ (b) Filling $x = 0.50$

Figure 3.6: Graphic representation of a square lattice of 36 sites whose average concurrence has been optimized to a) A quarter of filling and b) Half filling

other three (separable state $|00\rangle$, $C = 0$). Thus, the average Concurrence for each site is $1/4$.

For band fillings $x = 0.25$ and $x = 0.75$, each four-site electronic island in the system is in the state $|0001\rangle + |0010\rangle + |0100\rangle + |1000\rangle$ and $|1110\rangle + |1101\rangle + |1011\rangle + |0111\rangle$, respectively.

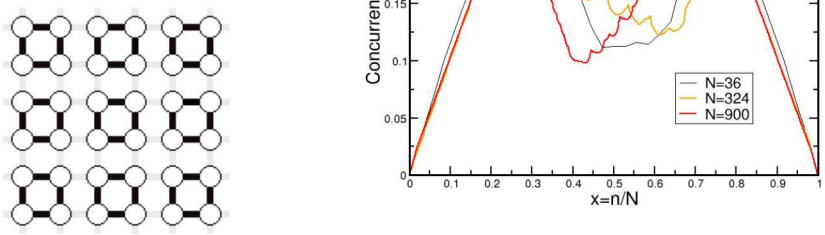

(a) Fixed employed pattern.

(b) Concurrence corresponding to the pattern in Fig. 3.7a

Figure 3.7: Behavior of average Concurrence for a square lattice configured as shown in fig. 3.7a. Three different sizes are shown: $N = 36$, $N = 100$ and $N = 900$.

To study in detail the system at electronic filling $x = 0.25$, we plotted the calculated average Concurrence for a fixed configuration similar to the one obtained in Fig. 3.6a. The two maxima are present at $x = 0.25$ and $x = 0.75$ but the system behaves differently elsewhere as the lattice size is incremented. This can be seen in Figure 3.7.

3.0.3 Triangular lattice

The triangular lattice is the first of the studied systems without bipartic-ity. How does these kind of system behaves under optimization?

The studied triangular lattice had 36 sites, and the effects of optimization under 3000 generations and a population size of 1500 can be seen in Figure 3.8. The higher number in population size is important in these kind of scenarios where finding an optimum solution is complicated by the lattice nature. A large population ensures enough diversity in solutions, which is key to prevent the algorithm to get stuck in local maxima.

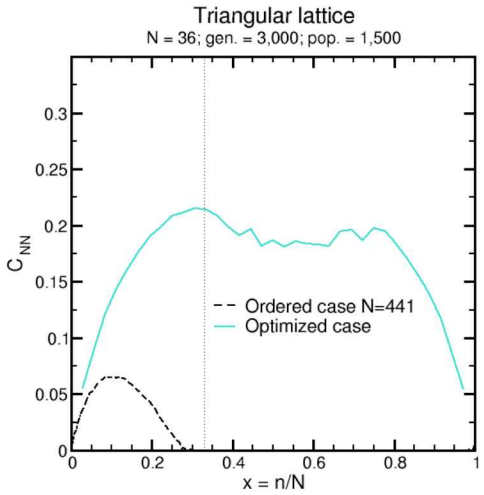

Figure 3.8: Behavior of Concurrence for a triangular lattice. Ordered and optmized cases.

Once again, it is possible to see the advantage of using an optimization technique. There is only one maximum at $x = 1/3$ although one would intuitively expect another at $x = 2/3$.

Is there any evidence that hint a possible transitions to a patterned configuration? In Figure 3.9 we show two interesting configurations corresponding to local maxima at $x = 0.33$ ($C = 0.2142$) and $x = 0.69$ ($C = 0.1960$).

Figure 3.9a definitely shows a pattern. In the case of Fig. 3.9b, the presence of a diamond pattern is only hinted at. We wondered what Concurrence could be obtained by testing lattices with fixed configurations based on these patterns. Three different designs were proposed, which can be seen in Figure 3.10.

We investigated which pattern the system preferred by running the optimization procedure but this time, when starting for each value of electronic filling, a hundred individuals where initialized to 0, a hundred to -5.0 and the rest with one of the proposed patterns. Results are shown in Fig. 3.11

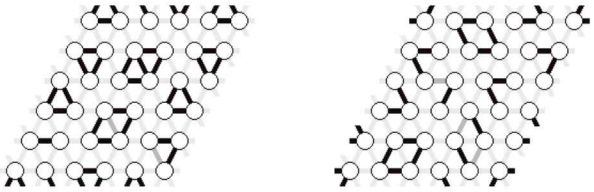

(a) Filling $x = 0.33$ (b) Filling $x = 0.69$

Figure 3.9: Configurations for the triangular lattice corresponding to local maxima obtained by the optimization procedure.

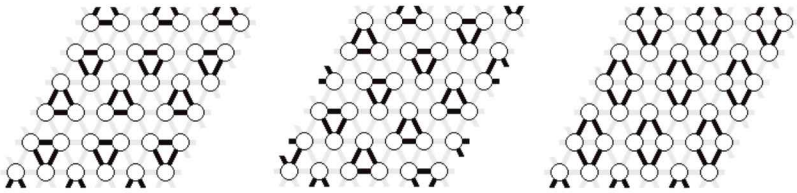

(a) “Triangle 1” (b) “Triangle 2” (c) “Diamond”

Figure 3.10: Lattice configurations based on Figs. 3.9a and 3.9b

(designs “Triangle 1” and “Triangle 2” yield identical results, and only the Concurrence for the “Triangle 2” design is included).

The best curve is a combination of several cases. Most points correspond to the case where the system was initialized with the design labeled “Triangle 2” (Fig. 3.10b); interestingly, that designs does not dominate the entire curve, as some poins are contributed by the case initialized with the “Diamond” setup. The values of average Concurrence are almost equal for the start and end of the curve, but some of them are contributed by the initial optimized case.

3.0.4 Betts lattice

The so-called Maple Leaf, or Betts lattice is also non-bipartite, and has less average triangular links than the triangular lattice.

With the experience of the triangular lattice, a first run was held for a lattice of $N = 54$ sites with 3000 generations and a population size of 1200 individuals. Then, taking the chromosome representing the best Concurrence a proposed lattice configuration is proposed (See Figs. 3.12).

With a setup as that of Fig. 3.12b, the optimizing procedure was run in a similar fashion as with the triangular lattice: a hundred individuals initialized to 0.0, a hundred to -5.0 and the others with the proposed setup. The final result is better than the randomly initialized case. This can be

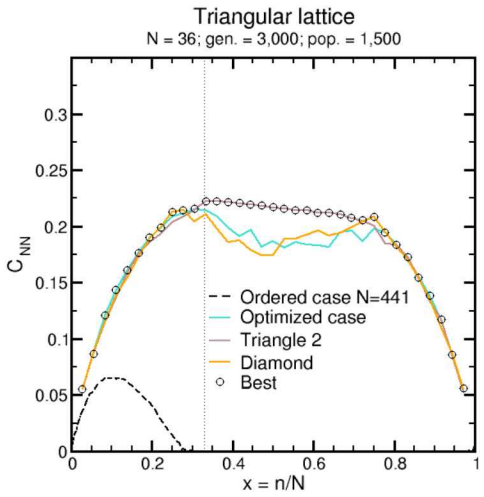

Figure 3.11: Triangular lattice combining results from different cases. The "best" curve represents the highest Concurrence for each filling.

seen on Figure 3.12c.

3.0.5 Kagome lattice

The last studied non-bipartite lattice is also the one with lesser number of neighbors.

As in the previous cases, a general optimization run was performed. The lattice had $N = 48$ sites and the algorithm was run using 3000 generations and 1200 individuals. The first results for this lattice comparing with the ordered case can be seen in Figure 3.13a.

Once again, a setup is based on the best individual from the simple optimization run (see Fig. 3.14a).

As previously, we have noted that this double procedure (using the algorithm once for finding possible setup patterns, running again initializing with the proposed setup) yields good results. Both curves are compared in Fig.3.14b.

3.0.6 Summary of non-bipartite lattices

For non-bipartite lattices it is possible to note that successful system configurations involve the formation of islands in form of triangles. The three lattices analyzed present a global maximum when electronic filling represents one electron for each three sites. In such cases, each three-

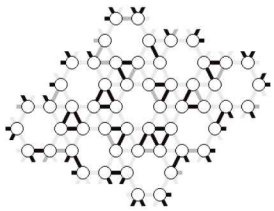

(a) Best individual for the Betts lattice using genetic algorithms ($x = 0.33$).

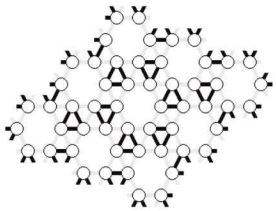

(b) Proposal based on 3.12a

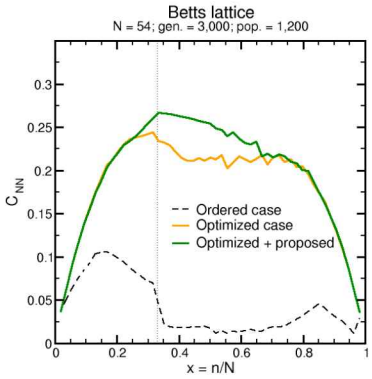

(c) Average nearest neighbor concurrence for the Betts lattice. Some individuals are now initialized as in Fig. 3.12b.

Figure 3.12: Graphic representation of a Betts lattice for 54 sites.

site (or qubit) subsystem share an electron and is in the state

$$|W\rangle = \frac{1}{3}\left(|001\rangle + |010\rangle + |100\rangle\right). \tag{3.2}$$

This tendency numerically supports the studies of Dür *et al.* [2], which propose that any three-qubit state $|\psi\rangle$ can be taken, using local operations, to one of only three different kind of state: a completely separable one, one in which only two qubits are entangled and another in which entanglement is maximum. The last class can be further classified in two states, the $|W\rangle$ and the $|GHZ\rangle$ ($|GHZ\rangle = 1/\sqrt{2}\left(|000\rangle + |111\rangle\right)$) states. The $|W\rangle$ states is the best of the two because it better preserves entanglement (i.e. is more "resilient") to qubit loss.

The number of nearest neighbors clearly impacts Concurrence. Figure 3.15 sums the results for the three non-bipartite lattices. It can be seen that systems with less nearest neighbors can be optimized to reach higher Concurrence values.

3.0.7 Quantum phase transitions

The quantum phase transition that the one dimensional system undergoes can be seen as a Peierls inestability (e.g. [6]), which occurs in metalic, one-dimensional systems where a change in structure in the unit cell leads to a decrease in kinetic energy. To study this phenomenon, the hopping elements t_{ij} were rewritten as $t_{2n,2n+1} = 1+\alpha$ and $t_{2n-1,2n} = 1-\alpha$,

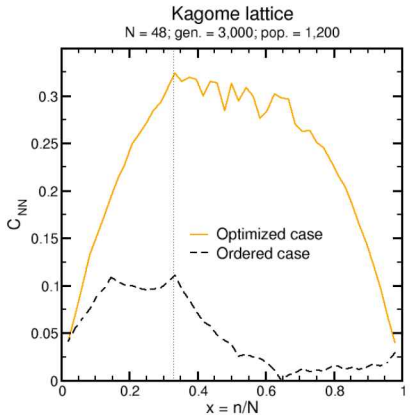

(a) First neighbor average Concurrence for a Kagome lattice as a function of electronic filling $x = n/N$. Ordered and optimized cases depicted.

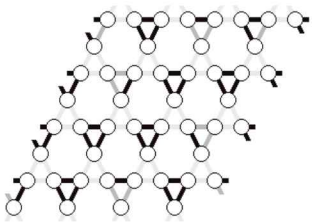

(b) Graphical representation of the best individual for the Kagome lattice, which was found at $x = 0.33$

Figure 3.13: First run optimizing the Kagome lattice.

where $0 \leq \alpha \leq 1$ is the dimerization parameter. In this manner it is possible to study the relationship between Concurrence and quantum phase transitions, for it is known [7] that a discontinuity (or singularity) in the ground state Concurrence (or its derivative) can be associated with a first (or second) phase transition, as long as artificial and accidental occurrences of non-analyticities in the ground-state are excluded.

The Concurrences for successive pairs of sites, $C_{2n,2n+1}$ and $C_{2n-1,2n}$ are shown in Figure 3.16, as well as their derivatives with respect to the dimerization parameter α. $C_{2n,2n+1} = 2.0\text{max}\{0, \gamma_{2n,2n+1} + \gamma_{2n,2n+1}^2 - 0.25\}$ and $C_{2n-1,2n} = 2.0\text{max}\{0, \gamma_{2n-1,2n} + \gamma_{2n-1,2n}^2 - 0.25\}$ [4], where $\gamma_{2n,2n+1} = \langle c_{2n}^\dagger c_{2n+1} \rangle$ and $\gamma_{2n-1,2n} = \langle c_{2n}^\dagger c_{2n} \rangle$ are the one-particle density-matrix elements or bond orders between nearest neighbors and can be calculated analytically [6]. These bond orders are continuous functions of α, the first one ranging from $\gamma_{2n,2n+1} = 0.318310$ ($\alpha = 0$) to 0.5 ($\alpha = 1.0$) and the second one from $\gamma_{2n-1,2n} = 0.318310$ ($\alpha = 0$) to 0.0 ($\alpha = 1.0$). Therefore, the discontinuity is artificial and comes from the particular definition of the Concurrence in equation 2.47.

On the other hand, the derivatives for $C_{2n,2n+1}$ and $C_{2n-1,2n}$ both present singularities at $\alpha \to 0$ (at the point of transition into a Peierls-like system). These can be associated with a *second order* Quantum Phase Transition.

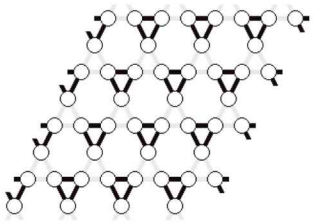

(a) Proposal based on Fig. 3.13b

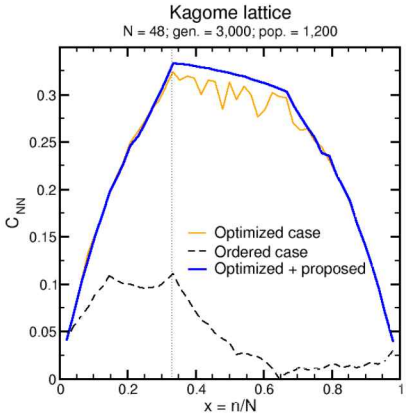

(b) Average Concurrence for the Kagome lattice. Blue line represents an optimized case initialized with some indiduals set as in Fig. 3.14a

Figure 3.14: Using the proposed setup (Fig. 3.13b), a higher value of Concurrence can be achieved in the optimization procedure.

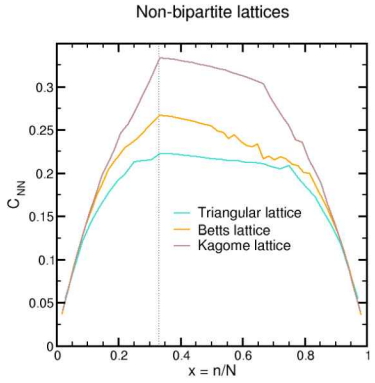

Figure 3.15: Comparación entre diferentes redes: Triangular ($N = 36$), Betts ($N = 54$) y Kagome ($N = 48$).

3.1 Conclusions

In the present work, the genetic algorithm technique was used to maximize the nearest-neighbor average Concurrence of several periodic systems by tuning the nearest-neighbor hopping integrals of a tight-binding Hamiltonian. The optimization of entanglement has been performed for one- and two-dimensional bipartite systems as well as for two-dimensional non-bipartite systems. The results show that the Concurrence of the optimized systems is very large in comparison with the ordered structures. This increase in the Concurrence is understood and interpreted by analyz-

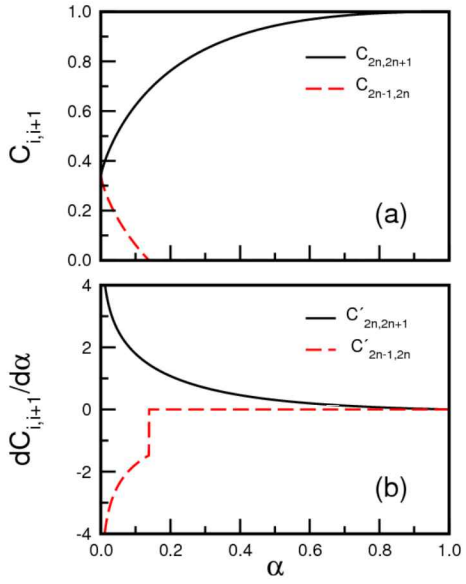

Figure 3.16: Concurrence $C_{2n,2n+1}$, $C_{2n-1,2n}$, and their derivatives.

ing the optimized nearest-neighbor hopping integrals. In general, we found certain tendencies of periodical systems to break into smaller subsystems. This is achieved in a natural manner by the system by making the hopping integrals evolve in such a way that the absolute value of some integrals is high in some cases ($|t_{ij}| \simeq 5$) and very small in others ($|t_{ij}| \leq 1$).

Using the results from the optimization procedure, new values for the hopping integrals are proposed, and each case is run for a second time, obtaining even higher values of Concurrence.

These results are related to the fact that quantum entanglement, in contrast with classical correlations, cannot be freely shared between many objects. This property –monogamy– is clearly noticeable in the case of the periodic ring at $x = 0.5$, where the nth site can be completely entangled with the next ($C_{2n,2n+1} \simeq 1$) while on the other hand it is almost unentangled with the preceding site ($C_{2n-1,2n} \simeq 0.1$). However, it is not necessary for the system to undergo a complete decoupling into isolated subsystems to have a large enhancement of entanglement with respect to the undistorted chain. A slight structural distortion brings already a considerable increase of the NN Concurrence, which continues growing and almost saturates when the ratio between the hopping integrals is about 10. Moreover, results at $x = 0.5$ show that, in order to maximize Concurrence, the system undergoes a structural transition.

Bibliography

[1] Valerie Coffman, Joydip Kundu, and William K. Wootters. Distributed entanglement. *Physical Review A*, 61(052306):1–5, 2000.

[2] W. Dür, G. Vidal, and J. I. Cirac. Three qubits can be entangled in two inequivalent ways. *Physical Review A*, 64(062314):1–12, November 2000.

[3] Shi-Jian Gu, Shu-Sa Deng, You-Quan Li, and Hai-Qing Lin. Entanglement and quantum phase transition in the extended hubbard model. *Physical Review Letters*, 93(8):1–4, 2004.

[4] Román López-Sandoval and Martin E. Garcia. Enhancement of nearest-neighbor entanglement in one-dimensional disordered systems. *Phys. Rev. B*, 74:174204, Nov 2006.

[5] Kevin M. O'Connor and William K. Wotters. Entangled rings. *Physical Review A*, A(052302):1–9, 2001.

[6] W. P. Su, J. R. Schrieffer, and A. J. Heeger. Soliton excitations in polyacetylene. *Physical Review B*, 22(4):2099–2111, August 1980.

[7] L.-A. Wu, M. S. Sarandy, and D. A. Lidar. Quantum phase transitions and bipartite entanglement. *Phys. Rev. Lett.*, 93:250404, Dec 2004.

[8] Paolo Zanardi. Quantum entanglement in fermionic lattices. *Physical Review A*, 65(042101):1–5, 2002.

Chapter 4

Entanglement in the Heisenberg Hamiltonian

4.1 Diagonalization of the Heisenberg Hamiltonian

As a natural step forward, our efforts have shifted towards using the techniques of concurrence optimization for the case of systems modeled by a general Heisenberg Hamiltonian of the form:

$$
\begin{aligned}
H &= \sum_{i \neq j} J_{i,j}\, \mathbf{S}_i \cdot \mathbf{S}_j = \sum_{i \neq j} J_{i,j} \left[S_i^x S_j^x + S_i^y S_j^y + S_i^z S_j^z \right] \\
H &= \frac{1}{2} \sum_{i \neq j} J_{i,j} \left[\left(S_i^+ S_j^- + S_i^- S_j^+ \right) + \frac{\left(n_{i\uparrow} - n_{i\downarrow} \right) \left(n_{j\uparrow} - n_{j\downarrow} \right)}{2} \right] \\
&= \frac{1}{2} \sum_{i \neq j} J_{i,j} \left[\left(S_i^+ S_j^- + S_i^- S_j^+ \right) + \frac{n_{i\uparrow} n_{j\uparrow} - n_{i\uparrow} n_{j\downarrow} - n_{i\downarrow} n_{j\uparrow} + n_{i\downarrow} n_{j\downarrow}}{2} \right] \\
&= \frac{1}{2} \sum_{i \neq j} J_{i,j} \left[\left(S_i^+ S_j^- + S_i^- S_j^+ \right) + \frac{\left(n_{i\uparrow} n_{j\uparrow} + n_{i\downarrow} n_{j\downarrow} \right)}{2} - \frac{\left(n_{i\uparrow} n_{j\downarrow} + n_{i\downarrow} n_{j\uparrow} \right)}{2} \right]
\end{aligned}
\tag{4.1}
$$

with $S_i^+ = S_i^x + iS_i^y = \hat{c}_{i\uparrow}^\dagger \hat{c}_{i\downarrow}$, $S_i^- = S_i^x - iS_i^y = \hat{c}_{i\downarrow}^\dagger \hat{c}_{i\uparrow}$, $S_i^z = (\hat{n}_{i\uparrow} - \hat{n}_{i\downarrow})/2$, $n_{i\sigma} = \hat{c}_{i\sigma}^\dagger \hat{c}_{i\sigma}$, the indices i, j representing each site in the system. J_{ij} is the exchange interaction between two spins in different sites and, depending if it is positive or negative, account for ferromagnetic or antiferromagnetic interactions, respectively.

In this Hamiltonian, one electron is localized on each site and can be found in any of the states $|\uparrow\rangle, |\downarrow\rangle$. These states are represented as a

binary 1 or 0.

It is well known that this Hamiltonian conmutes with the total spin-projection operator, $S_z = \sum_i (\hat{n}_{i\uparrow} - \hat{n}_{i\downarrow})/2$, and the $\mathbf{S}^2 = \sum_i (S_i^x S_i^x + S_i^y S_i^y + S_i^z S_i^z)$ operator as well (i.e., $[H, S_z] = 0$ and $[H, \mathbf{S}^2] = 0$). Therefore, it is possible to show, using the ladder operators $S^+ = \sum_i S_i^+$ and $S^- = \sum_i S_i^-$, that for each defined $|\mathbf{S}|$ there exist $2|\mathbf{S}| + 1$ degenerated eigenfunctions with degenerated eigenvalues $S_z = -|\mathbf{S}|, -|\mathbf{S}|+1 \ldots |\mathbf{S}|-1, |\mathbf{S}|$. To reduce the search space, we can make use of base functions which include these symmetries. For example, it is possible to use basis states with a fixed total spin S_z in order to diagonalize sector-by-sector. It is easy to see that all eigenfunctions with a defined $\mathbf{S}$ have an eigenfunction with an eigenvalue $S_z = 0$, and once calculated, the other $2|\mathbf{S}|$ eigenfunctions can be obtained by using ladder operators. For this reason, to choose base states with a total spin $S_z = 0$ ensures that the ground state obtained after finishing the diagonalization process is truly the lowest-energy state.

4.1.1 The basis

For a system of N sites, the total number of possible states is simply 2^N. In order to generate all the base states, we can realize that states represented by a binary number lesser than $|(0 \times N/2) \otimes (1 \times N/2)\rangle$ and greater than $|(1 \times N/2) \otimes (0 \times N/2)\rangle$ do not satisfy the $\hat{S}_z = 0$ restriction and can thus be discarded.

For example, for a $N = 4$ system, the basis states are

$$\begin{aligned} |1\rangle &= |0011\rangle \\ |2\rangle &= |0101\rangle \\ |3\rangle &= |0110\rangle \\ |4\rangle &= |1001\rangle \\ |5\rangle &= |1010\rangle \\ |6\rangle &= |1100\rangle. \end{aligned} \tag{4.2}$$

where states represented with a binary number lower than 3 (0011) or higher than 12 (1100) are forbidden because of the restriction.

The total number of permitted states (N_S) can be found to be $\frac{N!}{(N/2)!(N/2)!}$ (the permutation of N numbers, $N!$, discarding all the possible permutations of repeated numbers, in this case, all permutations of 0's and 1's).

4.1.2 The Hamiltonian Matrix

The matrix representation of the Hamiltonian grows very quickly. Although the matrix is Hermitian and it is only necessary to store the information of one triangular ($N_S^2/2 + N_S$), the size of said triangular for the case $N = 16$ ($N_S = 12,870$) is $82,824,885$ which takes aproximately 631 Megabytes using 8-byte real numbers. For $N = 18$ the number goes up to 9 Gigabytes which is already prohibitive for most day-to-day computers. This sets limits as to what is the maximum number of allowed sites in order for the system to be studied with this approach.

On the other hand, it is possible to use methods such as the Lanczos Algorithm where the memory requirements decrease considerably and is still possible to have meaningful results.

In the next sections, we will revise the characteristics of an efficiently-packed Hamiltonian, the calculation of its elements, and methods used to solve it.

The interaction matrix

Firstly, we define an interaction matrix J_{ij} which describes the degree of overlap between the wave functions of two sites. Because the overlap between sites $i - j$ is the same as the overlap between $j - i$, we need only to store the triangular of the matrix (we use the upper-triangular):

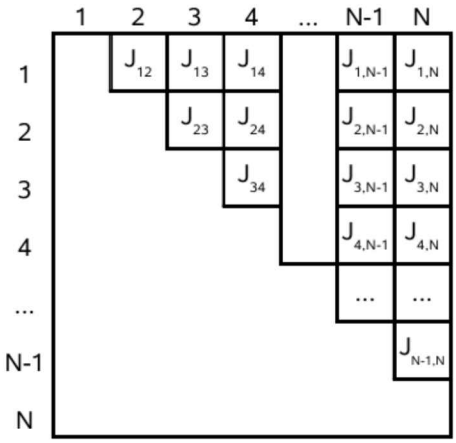

Thus, in order to use the value of a particular interaction element, we may instead reference the index that points to the data stored in J_{ij} (e.g. $J_{ij}[5] = J_{24}$). This allows us to employ 2-byte integers instead of 8-byte real numbers.

4.1.3 The non-diagonal elements

Each element in the upper triangular can be obtained by calculating $\langle\psi_x|H|\psi_y\rangle$ with $|\psi_x\rangle, |\psi_y\rangle$ pairs of states from the basis. The Hamiltonian in Eq. (4.1) can be treated as the sum of two components:

$$H = H_{\text{I}} + H_{\text{II}} \tag{4.3}$$

$$H_{\text{I}} = \frac{1}{2}\sum_{i\neq j} J_{i,j}\left(S_{i^+}S_{j^-} + S_{i^-}S_{j^+}\right) \tag{4.4}$$

$$H_{\text{II}} = \frac{1}{4}\sum_{i\neq j} J_{i,j}\left[\left(n_{i\uparrow}n_{j\uparrow} + n_{i\downarrow}n_{j\downarrow}\right) - \left(n_{i\uparrow}n_{j\downarrow} + n_{i\downarrow}n_{j\uparrow}\right)\right] \tag{4.5}$$

We will focus now on those elements off the main diagonal ($y > x$).

The second part, Eq. (4.5) is composed of number operators which do not modify the states they are operating on. Remember that $n_{i\uparrow} = \hat{c}^\dagger_{i\uparrow}\hat{c}_{i\uparrow}$ so $n_{i\uparrow}$ actually represents whether a particle is found in the state $\uparrow$ at the i site.

If the states remain unchanged they will vanish due to orthogonality (remember that non-diagonal elements are obtained by using different bra's and ket's). This means that, for the non-diagonal elements, we need only focus on the first part, Eq. (4.4), of the Hamiltonian.

Equation (4.4),

$$\sum_{i\neq j} J_{i,j}\left(S^+_i S^-_j + S^-_i S^+_j\right), \tag{4.6}$$

basically switches the state between sites i and j if (and only if) they are different (remember that $S^+_i = \hat{c}^\dagger_{i\uparrow}\hat{c}_{i\downarrow}$ and $S^-_i = \hat{c}^\dagger_{i\downarrow}\hat{c}_{i\uparrow}$). This means that the Hamiltonian takes the ket at the right and mixes it in as many states as elements are in the summatory. Nevertheless, when carefully analyzed, it becomes clear that every one of the states from this combination except one, vanish due to orthogonality. In other words, there exists at most one and only one permutation between two different states.

In our early example of $N = 4$ the element H_{12} is:

$$\langle 1|H|2\rangle \tag{4.7}$$

$$= \langle 1|H_{\text{I}} + H_{\text{II}}|2\rangle. \tag{4.8}$$

As discussed before, the second part of H does not change the ket and all those cases are discarded due to orthogonality. Therefore

$$H_{12} = \langle 1|H_{\text{I}}|2\rangle \tag{4.9}$$

$$= \langle 0011|\sum_{i\neq j} J_{i,j}\left(S^+_i S^-_j + S^-_i S^+_j\right)|0101\rangle \tag{4.10}$$

Suppose that the summation order is $(1,2),(1,3),(2,3),(1,4),(2,4),(3,4)$ (without repetitions). Then

$$\begin{aligned}\langle 0011|H_{\mathrm{I}}|0101\rangle = \\ &\langle 0011|J_{12}\left(S_1^+S_2^- + S_1^-S_2^+\right) + J_{13}\left(S_1^+S_3^- + S_1^-S_3^+\right) \\ &+ J_{23}\left(S_2^+S_3^- + S_2^-S_3^+\right) + J_{14}\left(S_1^+S_4^- + S_1^-S_4^+\right) \\ &+ J_{24}\left(S_2^+S_4^- + S_2^-S_4^+\right) + J_{34}\left(S_3^+S_4^- + S_3^-S_4^+\right)|0101\rangle\end{aligned} \tag{4.11}$$

$$\begin{aligned}=&\langle 0011|J_{12}S_1^+S_2^- + J_{12}S_1^-S_2^+ + J_{13}S_1^+S_3^- + J_{13}S_1^-S_3^+ \\ &+ J_{23}S_2^+S_3^- + J_{23}S_2^-S_3^+ + J_{14}S_1^+S_4^- + J_{14}S_1^-S_4^+ \\ &+ J_{24}S_2^+S_4^- + J_{24}S_2^-S_4^+ + J_{34}S_3^+S_4^- + J_{34}S_3^-S_4^+|0101\rangle.\end{aligned} \tag{4.12}$$

Each operator acts on the ket, yielding:

$$\begin{aligned}&J_{12}S_1^+S_2^-|0101\rangle \to 0 \\ &J_{12}S_1^-S_2^+|0101\rangle \to J_{12}S_1^-|0111\rangle \to J_{12}|0110\rangle \\ &J_{13}S_1^+S_3^-|0101\rangle \to J_{13}S_1^+|0001\rangle \to 0 \\ &J_{13}S_1^-S_3^+|0101\rangle \to 0 \\ &J_{23}S_2^+S_3^-|0101\rangle \to J_{23}S_2^+|0001\rangle \to J_{23}|0011\rangle \\ &J_{23}S_2^-S_3^+|0101\rangle \to 0 \\ &J_{14}S_1^+S_4^-|0101\rangle \to 0 \\ &J_{14}S_1^-S_4^+|0101\rangle \to J_{14}S_1^-|1101\rangle \to J_{14}|1100\rangle \\ &J_{24}S_2^+S_4^-|0101\rangle \to 0 \\ &J_{24}S_2^-S_4^+|0101\rangle \to J_{24}S_2^-|1101\rangle \to 0 \\ &J_{34}S_3^+S_4^-|0101\rangle \to 0 \\ &J_{34}S_3^-S_4^+|0101\rangle \to J_{34}S_3^-|1101\rangle \to J_{34}|1001\rangle\end{aligned} \tag{4.13}$$

And thusly, $\langle 0011|H_{\mathrm{I}}|0101\rangle$ becomes

$$\begin{aligned}=&\langle 0011|(J_{12}|0110\rangle + J_{23}|0011\rangle + J_{14}|1100\rangle \\ &+ J_{34}|1001\rangle) \\ =&\langle 1|\left(J_{12}|3\rangle + J_{23}|1\rangle + J_{14}|6\rangle + J_{34}|4\rangle\right) \\ =&J_{12}\langle 1|3\rangle + J_{23}\langle 1|1\rangle + J_{14}\langle 1|6\rangle + J_{34}\langle 1|4\rangle \\ =&J_{23}\end{aligned} \tag{4.14}$$

Where we are considering that the first site is at the *right* side of its representation (we have changed from the traditional left-hand side in multiple-qubit systems because when manipulating the representations with traditional bitwise operations, the least significant bit is at the right). In this

example, we can see that the only meaningful permutation *connecting* the states is the one associated with J_{23}. This characteristic can be exploited for calculating all the other non-zero elements stored in the auxiliary matrix `llenar`. As mentioned before, we store not the actual value of the table J_{ij} but rather the *index* pointing to the value in the table.

Calculating the non-diagonal elements

We make use of the fact that only one J_{ij} is needed in each non-diagonal element. If a particular J_{ij} is non-zero, it means that the spin-flip between the sites i, j will connect two different basis states. Consider the following simple example with $N = 4$:

		$\|1\rangle$ $\|0011\rangle$	$\|2\rangle$ $\|0101\rangle$	$\|3\rangle$ $\|0110\rangle$	$\|4\rangle$ $\|1001\rangle$	$\|5\rangle$ $\|1010\rangle$	$\|6\rangle$ $\|1100\rangle$
$\|1\rangle$	$\|0011\rangle$	D_1	J_{23}	J_{13}	J_{24}	J_{14}	-
$\|2\rangle$	$\|0101\rangle$		D_2	J_{12}	J_{34}	-	J_{14}
$\|3\rangle$	$\|0110\rangle$			D_3	-	J_{34}	J_{24}
$\|4\rangle$	$\|1001\rangle$				D_4	J_{12}	J_{13}
$\|5\rangle$	$\|1010\rangle$					D_5	J_{23}
$\|6\rangle$	$\|1100\rangle$						D_6

As we move to larger systems, the Hamiltonian matrix becomes sparser. Here is the case for $N = 6$:

	$\|1\rangle$ $\|000 111\rangle$	$\|2\rangle$ $\|001 011\rangle$	$\|3\rangle$ $\|001 101\rangle$	$\|4\rangle$ $\|001 110\rangle$	$\|5\rangle$ $\|010 011\rangle$	$\|6\rangle$ $\|010 101\rangle$	$\|7\rangle$ $\|010 110\rangle$	$\|8\rangle$ $\|011 001\rangle$	$\|9\rangle$ $\|011 010\rangle$	$\|10\rangle$ $\|011 100\rangle$	$\|11\rangle$ $\|100 011\rangle$	$\|12\rangle$ $\|100 101\rangle$	$\|13\rangle$ $\|100 110\rangle$	$\|14\rangle$ $\|101 001\rangle$	$\|15\rangle$ $\|101 010\rangle$	$\|16\rangle$ $\|101 100\rangle$	$\|17\rangle$ $\|110 001\rangle$	$\|18\rangle$ $\|110 010\rangle$	$\|19\rangle$ $\|110 100\rangle$	$\|20\rangle$ $\|111 000\rangle$
$\|1\rangle\|000111\rangle$	D_1	J_{34}	J_{24}	J_{14}	J_{35}	J_{25}	J_{15}	-	-	-	J_{36}	J_{26}	J_{16}	-	-	-	-	-	-	-
$\|2\rangle\|001011\rangle$		D_2	J_{23}	J_{13}	J_{45}	-	-	J_{25}	J_{15}	-	J_{46}	-	-	J_{26}	J_{16}	-	-	-	-	-
$\|3\rangle\|001101\rangle$			D_3	J_{12}	-	J_{45}	-	J_{35}	-	J_{15}	-	J_{46}	-	J_{36}	-	J_{16}	-	-	-	-
$\|4\rangle\|001110\rangle$				D_4	-	-	J_{45}	-	J_{35}	J_{25}	-	-	J_{46}	-	J_{36}	J_{26}	-	-	-	-
$\|5\rangle\|010011\rangle$					D_5	J_{23}	J_{13}	J_{24}	J_{14}	-	J_{56}	-	-	-	-	-	J_{26}	J_{16}	-	-
$\|6\rangle\|010101\rangle$						D_6	J_{12}	J_{34}	-	J_{14}	-	J_{56}	-	-	-	-	J_{36}	-	J_{16}	-
$\|7\rangle\|010110\rangle$							D_7	-	J_{34}	J_{24}	-	-	J_{56}	-	-	-	-	J_{36}	J_{26}	-
$\|8\rangle\|011001\rangle$								D_8	J_{12}	J_{13}	-	-	-	J_{56}	-	-	J_{46}	-	-	J_{16}
$\|9\rangle\|011010\rangle$									D_9	J_{23}	-	-	-	-	J_{56}	-	-	J_{46}	-	J_{26}
$\|10\rangle\|011100\rangle$										D_{10}	-	-	-	-	-	J_{56}	-	-	J_{46}	J_{36}
$\|11\rangle\|100011\rangle$											D_{11}	J_{23}	J_{13}	J_{24}	J_{14}	-	J_{25}	J_{15}	-	-
$\|12\rangle\|100101\rangle$												D_{12}	J_{12}	J_{34}	-	J_{14}	J_{35}	-	J_{15}	-
$\|13\rangle\|100110\rangle$													D_{13}	-	J_{34}	J_{24}	-	J_{35}	J_{25}	-
$\|14\rangle\|101001\rangle$														D_{14}	J_{12}	J_{13}	J_{45}	-	-	J_{15}
$\|15\rangle\|101010\rangle$															D_{15}	J_{23}	-	J_{45}	-	J_{25}
$\|16\rangle\|101100\rangle$																D_{16}	-	-	J_{45}	J_{35}
$\|17\rangle\|110001\rangle$																	D_{17}	J_{12}	J_{13}	J_{14}
$\|18\rangle\|110010\rangle$																		D_{18}	J_{23}	J_{24}
$\|19\rangle\|110100\rangle$																			D_{19}	J_{34}
$\|20\rangle\|111000\rangle$																				D_{20}

A first approach would be to, for each entry in the Hamiltonian, apply a bit-by-bit XOR operation between the row- and column-states binary representation. If there are exactly two bits set to 1, then both states are connected by the Hamiltonian and the entry is non-zero.

Although this is a very straight forward method, it does not scale well with systems of considerable size, and we have yet to consider further restrictions such as allowing only certain interactions to be non-zero, which ultimately represent additional slow-downs.

We may now take another approach developed in this work, which, to the best of our knowledge, has not been employed previously. If a particular J_{ij} represents a pair of basis states connected through a spin-flip operation, then it is possible to form a set of connected states permutating the remaining spins from the bra and ket in the same manner. For example, if J_{13} represents a spin flip between fixed sites $1, 3$ connecting two states, then:

$$J_{13} \rightarrow \langle xxx\mathbf{1}x\mathbf{0}| - |xxx\mathbf{0}x\mathbf{1}\rangle \tag{4.15}$$

where all the x are fixed spin-site states. These should be equal among the bra and ket, and be represented by all the possible permutations of spins (computationally, 0's and 1's). *Said permutations are nothing more than the basis of the $N-2$ system*:

$$\begin{aligned} J_{13}&: \\ &0011 \rightarrow \langle \mathbf{00}1]\mathbf{1}[0| - |\mathbf{00}1]\mathbf{1}[1\rangle \\ &0101 \rightarrow \langle \mathbf{01}0]\mathbf{1}[0| - |\mathbf{01}0]\mathbf{1}[1\rangle \\ &0110 \rightarrow \langle \mathbf{01}1]\mathbf{0}[0| - |\mathbf{01}1]\mathbf{0}[1\rangle \\ &1001 \rightarrow \langle \mathbf{10}0]\mathbf{1}[0| - |\mathbf{10}0]\mathbf{1}[1\rangle \\ &1010 \rightarrow \langle \mathbf{10}1]\mathbf{0}[0| - |\mathbf{10}1]\mathbf{0}[1\rangle \\ &1100 \rightarrow \langle \mathbf{11}0]\mathbf{0}[0| - |\mathbf{11}0]\mathbf{0}[1\rangle. \end{aligned} \tag{4.16}$$

In order to construct every non-zero, non-diagonal element of the Hamiltonian, we pair the basis states of the $N-2$ system with fixed spin values representing the spin-flip performed by the Hamiltonian, and assemble a special number with the representations. Continuing with our example,

$$\begin{aligned} J_{13}&: \\ &0011 \rightarrow \langle \mathbf{00}1]\mathbf{1}[0| - |\mathbf{00}1]\mathbf{1}[1\rangle \rightarrow 001110001011 \rightarrow 907 \\ &0101 \rightarrow \langle \mathbf{01}0]\mathbf{1}[0| - |\mathbf{01}0]\mathbf{1}[1\rangle \rightarrow 010110010011 \rightarrow 1427 \\ &0110 \rightarrow \langle \mathbf{01}1]\mathbf{0}[0| - |\mathbf{01}1]\mathbf{0}[1\rangle \rightarrow 011100011001 \rightarrow 1817 \\ &1001 \rightarrow \langle \mathbf{10}0]\mathbf{1}[0| - |\mathbf{10}0]\mathbf{1}[1\rangle \rightarrow 100110100011 \rightarrow 2467 \\ &1010 \rightarrow \langle \mathbf{10}1]\mathbf{0}[0| - |\mathbf{10}1]\mathbf{0}[1\rangle \rightarrow 101100101001 \rightarrow 2857 \\ &1100 \rightarrow \langle \mathbf{11}0]\mathbf{0}[0| - |\mathbf{11}0]\mathbf{0}[1\rangle \rightarrow 110100110001 \rightarrow 3377. \end{aligned} \tag{4.17}$$

The $1-0$ configuration is chosen for the right side such that that state has the greater decimal representation.

We then create the family of each non-zero element with its corresponding decimal representation as its label. See table 4.1 for an example supposing $J_{13}, J_{25}, J_{46} \neq 0$.

J_{13}		Label
$001[1]1[0]$	$001[0]1[1]$	$\rightarrow 907$
$010[1]1[0]$	$010[0]1[1]$	$\rightarrow 1427$
$011[1]0[0]$	$011[0]0[1]$	$\rightarrow 1817$
$100[1]1[0]$	$100[0]1[1]$	$\rightarrow 2467$
$101[1]0[0]$	$101[0]0[1]$	$\rightarrow 2857$
$110[1]0[0]$	$110[0]0[1]$	$\rightarrow 3377$

J_{25}		Label
$0[1]01[0]1$	$0[0]01[1]1$	$\rightarrow 1351$
$0[1]10[0]1$	$0[0]10[1]1$	$\rightarrow 1611$
$0[1]11[0]0$	$0[0]11[1]0$	$\rightarrow 1806$
$1[1]00[0]1$	$1[0]00[1]1$	$\rightarrow 3171$
$1[1]01[0]0$	$1[0]01[1]0$	$\rightarrow 3366$
$1[1]10[0]0$	$1[0]10[1]0$	$\rightarrow 3626$

J_{46}		Label
$[1]0[0]011$	$[0]0[1]011$	$\rightarrow 2251$
$[1]0[0]101$	$[0]0[1]101$	$\rightarrow 2381$
$[1]0[0]110$	$[0]0[1]110$	$\rightarrow 2446$
$[1]1[0]001$	$[0]1[1]001$	$\rightarrow 3161$
$[1]1[0]010$	$[0]1[1]010$	$\rightarrow 3226$
$[1]1[0]100$	$[0]1[1]100$	$\rightarrow 3356$

Table 4.1: "Families" of valid Hamiltonian elements represented with the same overlapping coefficient J_{ij}

The order in which each family element is taken from the tree and inserted into the storage array is given by the element's labels. The lowest label is the first element to be inserted in the array and so on (in the examples, the label is a simple number formed by two 6-bit numbers. In our working code, the label is an 8-byte integer). As we store the complete information of the Hamiltonian, we also have to consider the matrix elements corresponding to the main diagonal(see 4.2).

Now we need only to choose the lesser value from each family, and record the corresponding J_{ij} index. If a member of the diagonal family of elements is chosen, a dummy index is chosen (for example, 0) that will serve to indicate that a column has reached its end. We also keep track of which row corresponds to the particular value of the Hamiltonian. It can be easily obtained by masking the left-hand part of each family member:

$$J_{13}: \quad \underbrace{\langle \mathbf{001}[1]\mathbf{1}[0]|}_{\langle 4|} - |\mathbf{001}[0]\mathbf{1}[1]\rangle. \tag{4.18}$$

Storing this information will reveal its usefulness when matrix-vector multiplications appear for solving the Hamiltonian.

Diagonal		Label
000111	000111	$\rightarrow 455$
001011	001011	$\rightarrow 715$
001101	001101	$\rightarrow 845$
001110	001110	$\rightarrow 910$
010011	010011	$\rightarrow 1235$
010101	010101	$\rightarrow 1365$
010110	010110	$\rightarrow 1430$
011001	011001	$\rightarrow 1625$
011010	011010	$\rightarrow 1690$
011100	011100	$\rightarrow 1820$
100011	100011	$\rightarrow 2275$
100101	100101	$\rightarrow 2405$
100110	100110	$\rightarrow 2470$
101001	101001	$\rightarrow 2665$
101010	101010	$\rightarrow 2730$
101100	101100	$\rightarrow 2860$
110001	110001	$\rightarrow 3185$
110010	110010	$\rightarrow 3250$
110100	110100	$\rightarrow 3380$
111000	111000	$\rightarrow 3640$

Table 4.2: The diagonal elements for a $N = 6$ system.

As a sidenote, using this method also gives the exact formula to calculate the number of elements in the Hamiltonian:

$$\begin{aligned} N_{\mathsf{H}} &= (N_s(N-2))(J_{nz}) + N_s \\ &= \left(\frac{(N-2)!}{\left(\frac{N-2}{2}\right)!\left(\frac{N-2}{2}\right)!}\right)(J_{nz}) + \left(\frac{(N)!}{\left(\frac{N}{2}\right)!\left(\frac{N}{2}\right)!}\right) \\ &= \binom{N-2}{\frac{N-2}{2}}(J_{nz}) + \binom{N}{\frac{N}{2}} \end{aligned} \tag{4.19}$$

with J_{nz} the number of non-zero elements to be considered from the overlapping matrix. This number will depend upon the geometry of the system.

4.1.4 Main diagonal elements

When considering elements in the main diagonal, that is, $\langle x|H|x\rangle$, it can be inferred from the previous section that the first part of the Hamiltonian, H_{I}, will mix the ket into many different orthogonal states and the resulting

states will vanish due to orthogonality. Thusly, we turn our attention to the second part of the Hamiltonian.

The second part of the Hamiltonian is stated in equation (4.5), namely

$$H_{\text{II}} = \sum_{i \neq j} J_{i,j} \left[(n_{i\uparrow} n_{j\uparrow} + n_{i\downarrow} n_{j\downarrow}) - (n_{i\uparrow} n_{j\downarrow} + n_{i\downarrow} n_{j\uparrow}) \right],$$

where the number operator n can be rewritten in terms of the creation and annihilation operators (e.g. $n_{x\uparrow} = c^{\dagger}_{x\uparrow} c_{x\uparrow}$). It is clear that, when H_{II} operates over the ket-states, it probes them in search of coincidence or difference in the spin of a pair i, j of sites, summing a J_{ij} term in the former case or substracting it in the latter. As an example, for an $N = 4$ system the first element $\langle 1|H|1\rangle$ is:

$$\langle 1|H|1\rangle = \langle 1|H_{\text{II}}|1\rangle = \langle 0011|H_{\text{II}}|0011\rangle \tag{4.20}$$

$$\begin{aligned}
=&\langle 0011| J_{12} \left[(n_{1\uparrow} n_{2\uparrow} + n_{1\downarrow} n_{2\downarrow}) - (n_{1\uparrow} n_{2\downarrow} + n_{1\downarrow} n_{2\uparrow}) \right] \\
&+ J_{13} \left[(n_{1\uparrow} n_{3\uparrow} + n_{1\downarrow} n_{3\downarrow}) - (n_{1\uparrow} n_{3\downarrow} + n_{1\downarrow} n_{3\uparrow}) \right] \\
&+ J_{23} \left[(n_{2\uparrow} n_{3\uparrow} + n_{2\downarrow} n_{3\downarrow}) - (n_{2\uparrow} n_{3\downarrow} + n_{2\downarrow} n_{3\uparrow}) \right] \\
&+ J_{14} \left[(n_{1\uparrow} n_{4\uparrow} + n_{1\downarrow} n_{4\downarrow}) - (n_{1\uparrow} n_{4\downarrow} + n_{1\downarrow} n_{4\uparrow}) \right] \\
&+ J_{24} \left[(n_{2\uparrow} n_{4\uparrow} + n_{2\downarrow} n_{4\downarrow}) - (n_{2\uparrow} n_{4\downarrow} + n_{2\downarrow} n_{4\uparrow}) \right] \\
&+ J_{34} \left[(n_{3\uparrow} n_{4\uparrow} + n_{3\downarrow} n_{4\downarrow}) - (n_{3\uparrow} n_{4\downarrow} + n_{3\downarrow} n_{4\uparrow}) \right] |0011\rangle
\end{aligned} \tag{4.21}$$

$$\begin{aligned}
=&\langle 0011| (J_{12}|0011\rangle - J_{13}|0011\rangle - J_{23}|0011\rangle - J_{14}|0011\rangle \\
&- J_{24}|0011\rangle + J_{34}|0011\rangle)
\end{aligned} \tag{4.22}$$

$$\begin{aligned}
=&J_{12}\langle 0011|0011\rangle - J_{13}\langle 0011|0011\rangle - J_{23}\langle 0011|0011\rangle \\
&- J_{14}\langle 0011|0011\rangle - J_{24}\langle 0011|0011\rangle + J_{34}\langle 0011|0011\rangle
\end{aligned} \tag{4.23}$$

$$=J_{12} - J_{13} - J_{23} - J_{14} - J_{24} + J_{34}. \tag{4.24}$$

As can be seen, the elements of the main diagonal are calculated as a summation over all pairs of valid J_{ij} elements, $\sum_{i<j}^{N} (-1)^{\alpha} J_{ij}$, with an additional coefficient α representing the different signs which depend upon the particular basis state the H_{II} Hamiltonian is operating on. For a $N = 6$ system, the sign table can be seen in table 4.3.

A first approach to calculating the diagonal elements consists in precalculating the signs for each element J_{ij}. Every time the actual value of the elements needs to be recalculated –say, if a different set of values for the J_{ij} elements is chosen at runtime–, a simple dot-product between the sign table and the J_{ij} would suffice. Due to the size of the resulting sign-matrix

($N_s \times J_{nz}$), we chose a different approach wich sacrifices a bit of speed in favor of memory efficiency.

The second approach consists in initializing the diagonal vector with a single value equal to $-\sum_{i<j} J_{ij}$. Now, for each state and pair i, j of sites, we need only compensate summing $2J_{ij}$ should the i and j sites are equal. This is accomplished by making a bit-by-bit `xor` operation over the basis state shifted i and j places to the right. If those bits are equal, the least significant bit is 0, so a `modulo 2` operation is sufficient to tell whether it is necessary to sum $2J_{ij}$.

Whichever technique is employed, a twofold improvement in performance can be made if one notices that the sign-matrix is symmetric with respect to the mid-states (that is, the first and last states have the same signs).

	J_{12}	J_{13}	J_{23}	J_{14}	J_{24}	J_{34}	J_{15}	J_{25}	J_{35}	J_{45}	J_{16}	J_{26}	J_{36}	J_{46}	J_{56}
000111	■	■	■	□	□	□	□	□	□	■	□	□	□	■	■
001011	■	□	□	■	■	□	□	□	■	□	□	□	■	□	■
001101	□	■	□	■	□	■	□	■	□	□	□	■	□	□	■
001110	□	□	■	□	■	■	■	□	□	□	■	□	□	□	■
010011	■	□	□	□	□	■	■	■	□	□	□	□	■	■	□
010101	□	■	□	□	■	□	■	□	■	□	□	■	□	■	□
010110	□	□	■	■	□	□	□	■	■	□	■	□	□	■	□
011001	□	□	■	■	□	□	■	□	□	■	□	■	■	□	□
011010	□	■	□	□	■	□	□	■	□	■	■	□	■	□	□
011100	■	□	□	□	□	■	□	□	■	■	■	■	□	□	□
100011	■	□	□	□	□	■	□	□	■	■	■	■	□	□	□
100101	□	■	□	□	■	□	□	■	□	■	■	□	■	□	□
100110	□	□	■	■	□	□	■	□	□	■	□	■	■	□	□
101001	□	□	■	■	□	□	□	■	■	□	■	□	□	■	□
101010	□	■	□	□	■	□	■	□	■	□	□	■	□	■	□
101100	■	□	□	□	□	■	■	■	□	□	□	□	■	■	□
110001	□	□	■	□	■	■	■	□	□	□	■	□	□	□	■
110010	□	■	□	■	□	■	□	■	□	□	□	■	□	□	■
110100	■	□	□	■	■	□	□	□	■	□	□	□	■	□	■
111000	■	■	■	□	□	□	□	□	□	■	□	□	□	■	■

Table 4.3: H_{II} applied over a general $N = 6$ system. Every square represents whether the corresponding J_{ij} element is added or substracted. Filled square: $+$, empty square: $-$

4.1.5 Lanczos

The diagonalization step was carried on using the Lanczos method, which is a specially suitable approach when dealing with very sparse matrices.

The Lanczos method is an iterative algorithm that generates a tridiagonal, symmetrical matrix T with the property that its extremal eigenvalues are progressively better estimates of the original matrix' extremal eigenvalues.

4.2 Concurrence of systems described by the Heisenberg Hamiltonian

The necessary formulas to calculate Concurrence C_{ij} are similar to those described in detail in the second chapter. We will briefly address and adapt them in order to use them in systems described by the Heisenberg Hamiltonian.

Generally, the ground state obtained after the diagonalization of the Hamiltonian can be written as:

$$\begin{aligned}|\psi_{gs}\rangle = |\psi_{AB}\rangle = &\sum_m a_m|\downarrow\downarrow\rangle_A \otimes |\psi_B^m\rangle + \sum_o b_o|\downarrow\uparrow\rangle_A \otimes |\psi_B^o\rangle \\ &+ \sum_p c_p|\uparrow\downarrow\rangle_A \otimes |\psi_B^p\rangle + \sum_q d_q|\uparrow\uparrow\rangle_A \otimes |\psi_B^q\rangle.\end{aligned} \tag{4.25}$$

where naturally subsystem A, comprised by the localized spins in the sites of interest i and j, has four possible states.

To obtain the reduced density matrix of the subsystem A it is necessary to perform the trace over system B. Using the same arguments explained previously, the only non-zero elements in the reduced density matrix are

$$\rho_A = \begin{pmatrix} \rho_{11} & 0 & 0 & 0 \\ 0 & \rho_{22} & \rho_{23} & 0 \\ 0 & \rho_{32} & \rho_{33} & 0 \\ 0 & 0 & 0 & \rho_{44} \end{pmatrix} \tag{4.26}$$

The first element of the matrix, ρ_{11}, can be calculated in the following way

$$\rho_{11} = \langle\psi_{gs}|\hat{n}_{i\downarrow}\hat{n}_{j\downarrow}|\psi_{gs}\rangle \tag{4.27}$$

where the operator product $\hat{n}_{i\downarrow}\hat{n}_{j\downarrow}$ finds all the elements of the type $|\downarrow\downarrow\rangle_A \otimes |\psi_B\rangle$. The other elements are obtained with the following operators:

$$\rho_{22} = \langle\psi_{gs}|\hat{n}_{i\downarrow}\hat{n}_{j\uparrow}|\psi_{gs}\rangle \tag{4.28}$$
$$\rho_{33} = \langle\psi_{gs}|\hat{n}_{i\uparrow}\hat{n}_{j\downarrow}|\psi_{gs}\rangle \tag{4.29}$$
$$\rho_{44} = \langle\psi_{gs}|\hat{n}_{i\uparrow}\hat{n}_{j\uparrow}|\psi_{gs}\rangle \tag{4.30}$$
$$\rho_{23} = \langle\psi_{gs}|S_i^+ S_j^-|\psi_{gs}\rangle \tag{4.31}$$
$$\rho_{32} = \langle\psi_{gs}|S_i^- S_j^+|\psi_{gs}\rangle \tag{4.32}$$

where, due to the hermiticity of ρ_A, $\rho_{23} = \rho_{32}^*$. Note from the mathematical expression of the elements in ρ_A that the Concurrence between two sites is related with its ground state spin correlation, i.e.

$$\begin{aligned}\langle\psi_{gs}|\mathbf{S}_i \cdot \mathbf{S}_j|\psi_{gs}\rangle =& \langle\psi_{gs}|(S_i^x S_j^x + S_i^y S_j^y + S_i^z S_j^z)|\psi_{gs}\rangle \\ =& \langle\psi_{gs}|(S_i^+ S_j^- + S_i^- S_j^+)/2 + S_i^z S_j^z|\psi_{gs}\rangle \\ =& (\rho_{23} + \rho_{32})/2 + (\rho_{11} + \rho_{44})/4 - (\rho_{22} + \rho_{33})/4\end{aligned} \tag{4.33}$$

Finally, to be able to use the Concurrence equation (Eq. (1.23)), we use the square roots of the lambda coefficients:

$$\sqrt{\lambda_a} = \sqrt{\rho_{22}\rho_{33}} - |\rho_{23}| \tag{4.34}$$
$$\sqrt{\lambda_b} = \sqrt{\rho_{22}\rho_{33}} + |\rho_{23}| \tag{4.35}$$
$$\sqrt{\lambda_c} = \sqrt{\rho_{11}\rho_{44}} \tag{4.36}$$
$$\sqrt{\lambda_d} = \sqrt{\rho_{11}\rho_{44}} \tag{4.37}$$

Notice that λ_b is the largest eigenvalue. Thus, the final formula becomes

$$C = \max\{0, \sqrt{\rho_{22}\rho_{33}} + |\rho_{23}| - \sqrt{\rho_{22}\rho_{33}} + |\rho_{23}| - \sqrt{\rho_{11}\rho_{44}} - \sqrt{\rho_{11}\rho_{44}}\} \tag{4.38}$$
$$C = \max\{0, 2|\rho_{23}| - 2\sqrt{\rho_{11}\rho_{44}}\} \tag{4.39}$$
$$C = 2\max\{0, |\rho_{23}| - \sqrt{\rho_{11}\rho_{44}}\} \tag{4.40}$$

Remarkably, the mathematical expression for the Concurrence is completely different from the spin correlation function. This implies that Concurrence is a kind of quantum correlation distinct from traditional correlation functions used in solid state physics used, for example, to study quantum phase transitions.

4.3 First results and perspectives

4.3.1 Concurrence in small Heisenberg systems

We first calculated the effect of boundary conditions and dimerization over Concurrence and the spin correlation function (S_{ij}) of the ground state in small four-site Heisenberg systems. A ring and a chain were studied, noting that the difference in number of neighbors has important consequences in the values of Concurrence and spin correlation.

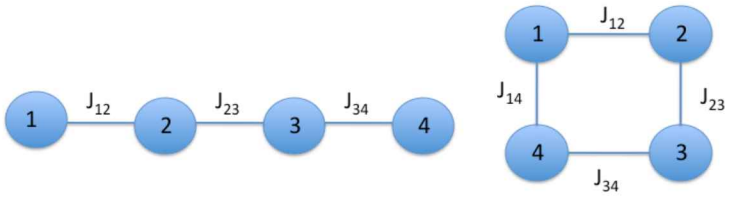

(a) Four site chain (b) Four site ring

Figure 4.1: First studies on small Heisenberg systems

In order to study the effects of dimerization, it is convenient to take into account that in the case of the four-site chain, the two strong and the two milder exchange interactions can be chosen arbitrarily, as long as they are intercalated. On the other hand, in the case of the four-site chain only three exchange interactions can be considered. In the following, the milder interaction is chosen as J_{23}.

In Fig. 4.2a, nearest-neighbor Concurrence (C_{12}, C_{23}) as a function of the dimerization factor is compared against spin correlation between the same neighbors in the ring system. The dimerization of the exchange interactions is as follows: $J_{12} = J_{34} = 1$ were kept constant while $J_{23} = J_{41} = 1 - \alpha$ decreases as a function of α.

From the figure, we can see that while the system is kept undimerized, Concurrence between distinct pairs of sites remains equal ($C_{12} = C_{23} = 0.5$), as well as their spin correlations. When the dimerization parameter is increased, C_{12} whose interaction exchange remained constant, starts increasing monotonously while C_{23} decreases until α reaches 0.5. Note that a possible discontinuity in the first derivative of C_{23} cannot be related to a quantum phase transition as it is due to the definition of Concurrence. On the other hand, both spin correlation functions show a continuous smooth behavior. Remarkably, $C_{12}(\alpha) > S_{12}(\alpha)$.

A notable effect on the loss of symmetry can be observed for the spin correlation functions in the four-site chain, which show different values

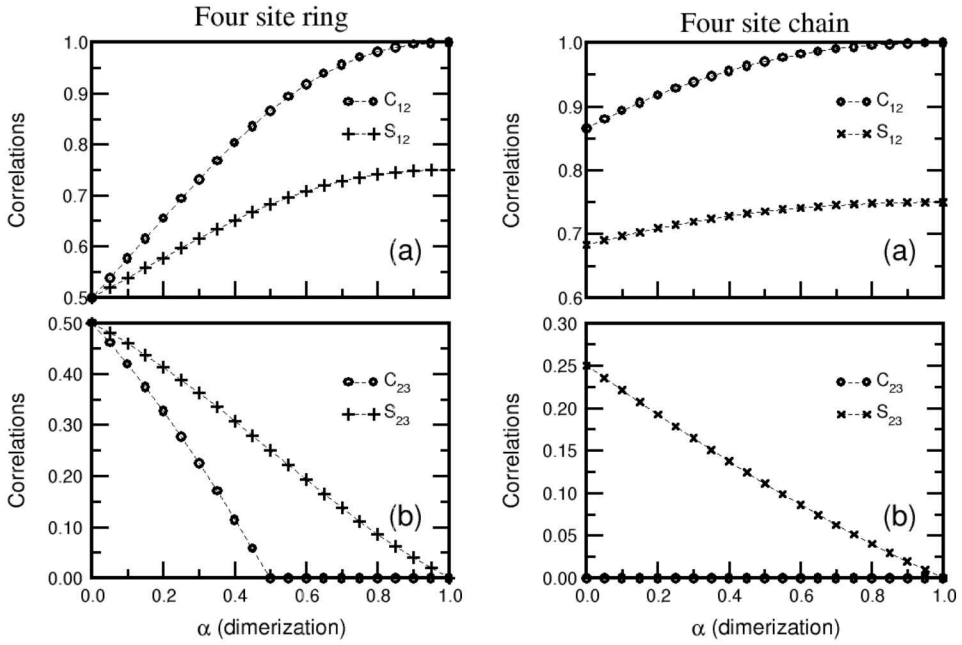

(a) Four site ring (b) Four site chain

Figure 4.2: Spin correlation and Concurrence for sites $1-2, 2-3$ in the four-site Heisenberg system

even in the undimerized case. Note also that C_{12} almost saturates for $\alpha = 0.866$. Naturally, the maximum is reached when the system is broken into two completely separated systems.

4.3.2 Heisenberg quantum switch

By tuning certain system's parameters, it could be possible, at least theoretically , to build a quantum switch that could move the quantum entanglement between two qubits from one state to the other. For example, Gao and Wang [4] propose a three-site Hubbard Hamiltonian with $N_e = 2$. They find two free parameters, U_0/t and U/t, which can be used as a tuning and control parameter, respectively. Depending on the sign and magnitude, the control parameter U/t can act as a barrier forbidding the double occupancy or act as an attractor freezing the two electrons on one site. When U/t is strongly posive Entanglement can be tuned between two saturation values using U_0/t. Although a physical implementation that could modify such system's parameters is unlikely, the idea inspired us to study the posibility of building a quantum switch in the Heisenberg model.

In Fig. 4.3a we show a possible scheme of quantum switch formed by a six-site ring. All exchange interactions are kept equal except for $J_{16} = 1-\alpha$,

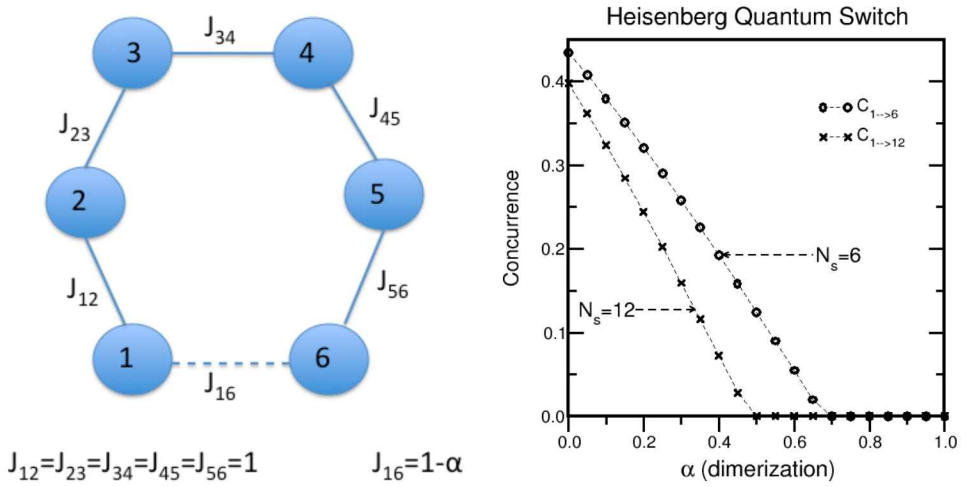

(a) Heisenberg hexagon. J_{ij} is the exchange interaction between spins of two sites.

(b) Four site chain

Figure 4.3: Turning off an on as a function of the dimerization parameter.

which will vary with the dimerization parameter α. This parameter will be responsible for turning off or on Concurrence C_{16}. Generally, the quantum switch can be realized using rings from different sizes, as can be seen in Fig. 4.3b. As in the six-site case, all exchange interactions of the twelve-site case are kept constant except for J_{1-12}. From the figure, we observe that the critical turning-on dimerization value α_{on} depends on the size of the system.

As for the viability of a practical physical realization, one possible approach could be to use coupled quantum dots after the ideas of Loss and DiVincenzo [5]. In their studies, the qubit is the spin of an excess electron in a quantum dot. They show that, for a pair of coupled quantum dots, the spin interactions between qubits can be manipulated by tuning the electrical tunneling barrier. If the potential barrier is high, tunneling is forbidden between dots; if it is lowered, spins can interact with a transient Heisenberg coupling

$$H(t) = J(t)\mathbf{S}_i \cdot \mathbf{S}_j \tag{4.41}$$

where $J(t) = 4t_0^2(t)/u$ dependes on the tunneling matrix parameter $t_0(t)$ and the charging energy u. $t_0(t)$ depends on the confinement voltage and, by modifying it, it is also possible to tune the value of $J(t)$.

Another possible alternative for the construction of a quantum switch is to employ optical lattices using ultra-cold atoms [3]. In this scheme, when atoms are confined in an optical lattice, the spin interaction can be

controlled adjusting the intensity, frequency and polarization of the laser being used. By tunning these parameters, a virtual tunneling control dependant of spin can be achieved, which in turn translates into a controlable Heisenberg exchange interaction.

4.3.3 Engineering of Concurrence

In order to realize some of the main quantum information tasks, it is necessary that a certain level of Entanglement exists between two qubits. For example, to use Entanglement as a quantum channel in order to exchange information, it is desirable that the particles which share Entanglement be apart from each other.

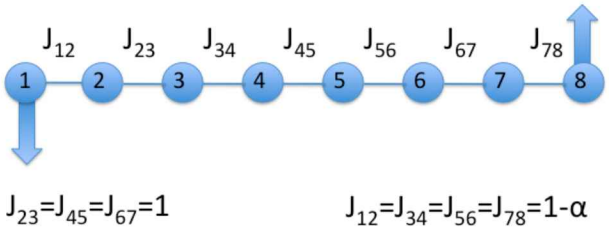

Figure 4.4: Eight-site Heisenberg chain.

Recently it has been shown [1] that in some spin models in the ground state, a couple of distant sites a and b can be highly entangled, even when those sites are separated by an infinite distance between them. This property is known as Long Distance Entanglement. Particularly, there is the spin $1/2$ Heisenberg chain where, even for mild dimerizations, non-local interactions can arise, that is, the outermost sites are entangled (see Fig. 4.4). This effect is due to the high symmetry of the ground state, which has to comply with the restriction $S_z = 0$. The effect can be understood as follows: as the dimerization increases, spins in sites $2-3$, $4-5$ and $6-7$ tend to form singlet states ($S^{\text{dim}} = 0, S_z^{\text{dim}} = 0$), which is the ground state for a Heisenberg dimer. To preserve $S_z = 0$, the outer spins 1 and 8 are forced into the singlet state, which shows maximum Concurrence.

The full behavior of the Heisenberg chain under alternating dimerization can be seen in Fig. 4.5, where chains of two sizes where studied. It can be seen that only a mild dimerization is necessary for the system to present high Concurence between its extremes. These are very interesting results for they show that an almost perfect entanglement between extremes does not depend on size, but rather on symmetry. This property could be exploited to its use in quantum teleportation.

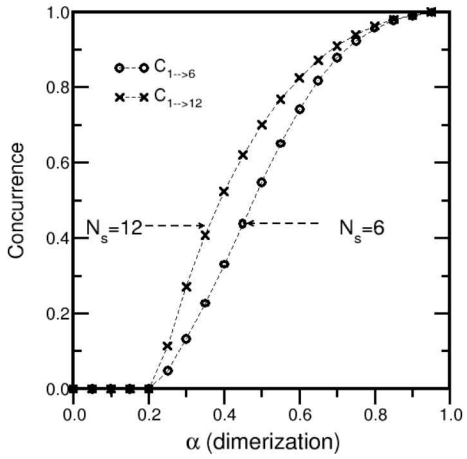

Figure 4.5: Effect of alternating dimerization on Heisenberg chains.

Unfortunately, the energy gap between the ground state and the first excited state in these kind of chains dissappears exponentially as the chain size increases. This means that even at low temperatures, the strong correlations between the spins at the extremes would loose their quantum coherence.

Due to these difficulties, new models have been studied where the gap decreases only algebraically. For example, Campos-Venuti *et al*. [2] studied two kinds of models: an open, dimerized XX chain, and an open XX chain with small end bonds. They find that the first model supports true long-distance Entanglement at zero temperature, while the second model supports “quasi-long-distance” Entanglement that slowly falls off with the size of the chain. The latter model is also better suited for quantum teleportation, as the energetic gap decreases only algebraically at moderately low temperatures.

4.3.4 Final thoughts and perspectives

Schemes such as quantum teleportation, which use a quantum channel to send information, can be realized in systems modeled with the Heisenberg model as the ones studied in the present chapter.

As future work, is it possible to keep investigating the possibility of finding system parameters which favor high end-to-end Entanglement as well as an energetic gap that does not decay exponentially. This could be worked on using the same methodology as the one employed in the previous chapters, namely, to use an optimization method such as genetic algorithms.

Bibliography

[1] L. Campos Venuti, C. Degli Esposti Boschi, and M. Roncaglia. Long-distance entanglement in spin systems. *Phys. Rev. Lett.*, 96:247206, Jun 2006.

[2] L. Campos Venuti, S. M. Giampaolo, F. Illuminati, and P. Zanardi. Long-distance entanglement and quantum teleportation in xx spin chains. *Phys. Rev. A*, 76:052328, Nov 2007.

[3] L.-M. Duan, E. Demler, and M. D. Lukin. Controlling spin exchange interactions of ultracold atoms in optical lattices. *Phys. Rev. Lett.*, 91:090402, Aug 2003.

[4] Jiming Gao and Jiaxiang Wang. A novel scheme for entanglement engineering in a fermionic system. arXiv:0803.0110v1, 2008.

[5] Daniel Loss and David P. DiVincenzo. Quantum computation with quantum dots. *Phys. Rev. A*, 57:120–126, Jan 1998.

Appendix A

Code details

A.1 Data arrays

In our program for solving a Heisenberg Hamiltonian, there exist several data-storing arrays and variables, whose type needs to be carefully chosen. Bracketed variables stand for an array.

- `N`: The size of the system.

- `imin, imax`: The lower- and upper-limit of the first and last states in the basis, in their binary representation.

- `estados_base`: The number of states in the basis, N_s. Calculated as $\binom{N}{N/2}$.

- `[da_representacion]`: Gives the binary representation of a basis state. For example, for $N = 6$, `da_representacion(1)`=000111=7 (the first state for the $N = 6$ case has the first three sites in the state $|1\rangle$ while the last three are in the state $|0\rangle$, this is represented in decimal notation as a 7, etc.).

- `[da_estado_vec]`: Given a binary representation of a system, the function `da_estado` returns the corresponding number of basis state. The actual mapping is done using an ancilliary matrix, `[da_estado_vec]`, which, to avoid wasting the first indices with representations lower than `imin` (discarded by the $S_z = 0$ restriction), stores the first basis state as its first element. The function simply shifts accordingly:

```
function da_estado(representacion)
        use data
        implicit none
```

```
        integer(4) :: da_estado, representacion

        da_estado = da_estado_vec(representacion-imin+1)

    end function da_estado
```

Special care is to be taken with representations outside the valid range of states, as no validation is made in order to speed calculations up.

- `[J_ij]`: Matrix storing the actual overlapping parameters. We only need store the elements corresponding to the upper triangular.

- `[llenar]`: Matrix storing information about the non-zero elements of the Hamiltonian. Each element is of type

```
TYPE :: hamiltoniano_empacado_elemento
        integer(2) :: J_ij
        integer(4) :: renglon
END TYPE
```

Where `J_ij` corresponds to an entry in `[J_ij]` and `renglon` is the corresponding row of this element in the Hamiltonian. Information about the column can be obtained indirectly by means of the `[diagonal]` matrix.

- `[diagonal]`: Matrix storing the values of the diagonal elements. Each element is of type

```
TYPE :: diagonal_elemento
        integer(4) :: posicion
        real(8) :: valor
END TYPE
```

with `posicion` representing its position in the `[llenar]` matrix and `valor` the actual, pre-calculated value of the element.

A representation of the Hamiltonian for the case $N = 4$ using the data structure just described is depicted in figure A.1.

A.2 Memory considerations

When coding a simulation that manipulates large amounts of data, it is important to take memory considerations into the code design in order to be as frugal as possible.

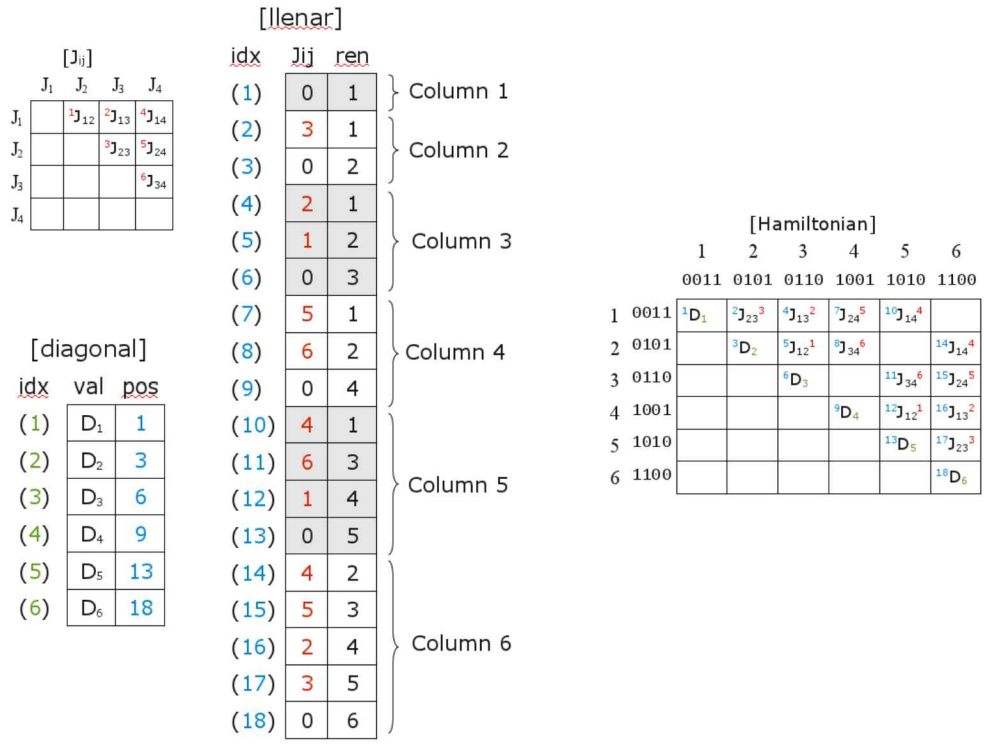

Figure A.1: The different arrays storing the information for the Hamiltonian.

A.2.1 The basis-storing arrays

Note that, for the case $N = 36$, the highest-valued representation corresponding to the last state in the basis is `11 11111111 11111110 00000000 00000000` (5 bytes), and would need an 8-byte integer in order to be addresseable (or a custom non-native 5-byte integer). In the case with $N = 34$, the numbers still fit in a 4-byte integer, but the most-significant bit is used for the sign and the roof value (the state represented as $|2, 333, 606, 220\rangle$) cannot be addressed in an array made from 4-byte integers (i.e. we cannot address a value stored in a *negative*-valued index). This makes the $N = 32$ the largest case provisioned in our program. The `imin` and `imax` values, as well as the auxiliary arrays `[da_representacion]` and `[estados_base]` can thusly be declared of kind `int(4)`.

N	$S[J_{ij}]$	$S_2[J_{ij}]$	$S_B[J_{ij}]$	N_s	bin	bytes
2	1	1	1	2	10	1
4	6	110	1	6	110	1
6	15	1111	1	20	10100	1
8	28	11100	1	70	1000110	1
10	45	101101	1	252	11111100	1
12	66	1000010	1	924	11 10011100	2
14	91	1011011	1	3,432	1101 01101000	2
16	120	1111000	1	12,870	110010 01000110	2
18	153	10011001	1	48,620	10111101 11101100	2
20	190	10111110	1	184,756	10 11010001 10110100	3
22	231	11100111	1	705,432	1010 11000011 10011000	3
24	276	1 00010100	2	2,704,156	101001 01000011 00011100	3
26	325	1 01000101	2	10,400,600	10011110 10110011 01011000	3
28	378	1 01111010	2	40,116,600	10 01100100 00100001 01111000	4
30	435	1 10110011	2	155,117,520	1001 00111110 11100111 11010000	4
32	496	1 11110000	2	601,080,390	100011 11010011 11000010 01000110	4
34	561	10 00110001	2	2,333,606,220	10001011 00011000 00000001 01001100	4*
36	630	10 01110110	2	9,075,135,300	10 00011100 11101011 10010011 01000100	5
38	703	10 10111111	2	35,345,263,800	1000 00111010 10111101 11101100 10111000	5
40	780	11 00001100	2	137,846,528,820	100000 00011000 01001011 00011011 00110100	5

Table A.1: $S[J_{ij}]$ the number of elements in the ovelapping matrix, $[J_{ij}]$. $S_2[J_{ij}]$ is the binary representation of $S[J_{ij}]$, $S_B[J_{ij}]$ are the minimum bytes necessary to store $S_2[J_{ij}]$. N_s is the number of states.

A.2.2 J_{ij}

With $N = 32$ the largest tractable system, the size of the array storing the values of the overlapping wavefunctions, $[J_{ij}]$, has a maximum of

$$\frac{N^2 - N}{2} = 496 \tag{A.1}$$

for the upper triangular. A 1-byte integer is too small to address such a number and thus we need an array declared with `int(2)`-type numbers.

A.2.3 The Hamiltonian upper triangular

N	size([da_estado])	bytes	Megabytes
2	1	4	
4	9	36	
6	49	196	
8	225	900	
10	961	3844	
12	3969	15876	
14	16129	64516	
16	65025	260100	
18	261121	1044484	0.996097565
20	1046529	4186116	3.99219131
22	4190209	16760836	15.9843788
24	16769025	67076100	63.9687538
26	67092481	268369924	255.937504
28	268402689	1073610756	1,023.875*
30	1073676289	4294705156	4,095.75
32	4294836225	17179344900	16,383.5

N	H_{total}	H_{total} binary bytes	
2	3	11	1
4	21	10101	1
6	210	11010010	1
8	2,485	1001 10110101	2
10	31,878	1111100 10000110	2
12	427,350	110 10000101 01010110	3
14	5,897,028	1011001 11111011 01000100	3
16	82,824,885	100 11101111 11001110 10110101	4
18	1,181,976,510	1000110 01110011 10000111 10111110	4
20	17,067,482,146	11 11111001 01001101 00011100 00100010	5
22	248,817,506,028	111001 11101110 10101101 11010110 11101100	5
24	3,656,231,188,246	11 01010011 01001000 01011100 01110111 00010110	6
26	54,086,245,380,300	110001 00110000 11101111 01110001 01110000 11001100	6
28	804,670,817,838,300	10 11011011 11011000 00000110 01000010 00100100 11011100	7

Table A.2: Size of the Hamiltonian's upper triangular. All elements.

N	Elements in [llenar]	binary	bytes
2	3	11	1
4	18	10010	1
6	110	1101110	1
8	630	10 01110110	2
10	3,402	1101 01001010	2
12	17,556	1000100 10010100	2
14	87,516	1 01010101 11011100	3
16	424,710	110 01111011 00000110	3
18	2,017,730	11110 11001001 11000010	3
20	9,422,556	10001111 11000110 11011100	3
22	43,384,068	10 10010101 11111101 00000100	4
24	197,403,388	1011 11000100 00100010 11111100	4
26	889,251,300	110101 00000000 11100101 11100100	4
28	3,971,543,400	11101100 10111000 11110001 01101000	4
30	17,605,838,520	100 00011001 01100011 11000110 10111000	5
32	77,539,370,310	10010 00001101 10110100 11100101 01000110	5

Table A.3: Size of `[llenar]` (all non-zero elements). The case for $N = 28$ cannot be indexed using four-byte integers because of the sign-bit

Appendix B

Quantum Gates

B.1 Quantum gates

In classical computation, manipulation of information is carried on logical gates, electronic devices made of transistors that allow the implementation of boolean algebra.

In quantum computation there exist also logic gates. From the mathematical point of view, the only condition needed is that the operators be unitary matrices (that is, $[\mathbf{A}][\mathbf{A}]^{\dagger} = \mathbf{I}$). We will briefly address some relevant quantum gates.

B.1.1 The NOT gate

The NOT gate is the basic one-bit gate, and its function is to change the present state for the other available state. In quantum computation, the equivalent gate interchanges the states' amplitudes. In matrix form, this gate is represented as

$$\mathbf{X} \equiv \begin{pmatrix} 0 & 1 \\ 1 & 0 \end{pmatrix} \tag{B.1}$$

such that, using the matrix representation of a qubit,

$$|\psi\rangle = \alpha|0\rangle + \beta|1\rangle = \begin{pmatrix} \alpha \\ \beta \end{pmatrix}, \tag{B.2}$$

we have

$$\mathbf{X}\begin{pmatrix} \alpha \\ \beta \end{pmatrix} = \begin{pmatrix} 0 & 1 \\ 1 & 0 \end{pmatrix}\begin{pmatrix} \alpha \\ \beta \end{pmatrix} = \begin{pmatrix} \beta \\ \alpha \end{pmatrix}. \tag{B.3}$$

B.1.2 Z Gate

This gate has the very simple task of changing the sign of the amplitude of the second state:

$$\mathbf{Z} \equiv \begin{pmatrix} 1 & 0 \\ 0 & -1 \end{pmatrix} \tag{B.4}$$

B.1.3 Hadamard gate

This gate mixes the state $|0\rangle$ into $(|0\rangle + |1\rangle)/\sqrt{2}$ and the state $|1\rangle$ into $(|0\rangle - |1\rangle)/\sqrt{2}$:

$$\mathbf{H} \equiv \frac{1}{\sqrt{2}} \begin{pmatrix} 1 & 1 \\ 1 & -1 \end{pmatrix} \tag{B.5}$$

B.1.4 Combining gates

For a two-qubit system, it is possible to combine one-qubit gates. For example, if we wish to use the NOT gate on the second qubit, we employ the $\otimes$ operation in order to combine the identity gate with the NOT gate:

$$\mathbf{I} \otimes \mathbf{X} \left(\alpha|00\rangle + \beta|01\rangle + \gamma|10\rangle + \delta|11\rangle\right) = \tag{B.6}$$

$$\begin{pmatrix} 1 & 0 \\ 0 & 1 \end{pmatrix} \otimes \begin{pmatrix} 0 & 1 \\ 1 & 0 \end{pmatrix} \begin{pmatrix} \alpha \\ \beta \\ \gamma \\ \delta \end{pmatrix} = \tag{B.7}$$

$$\begin{pmatrix} 1\begin{pmatrix} 0 & 1 \\ 1 & 0 \end{pmatrix} & 0\begin{pmatrix} 0 & 1 \\ 1 & 0 \end{pmatrix} \\ 0\begin{pmatrix} 0 & 1 \\ 1 & 0 \end{pmatrix} & 1\begin{pmatrix} 0 & 1 \\ 1 & 0 \end{pmatrix} \end{pmatrix} \begin{pmatrix} \alpha \\ \beta \\ \gamma \\ \delta \end{pmatrix} \tag{B.8}$$

and the operation is then

$$\begin{pmatrix} 0 & 1 & 0 & 0 \\ 1 & 0 & 0 & 0 \\ 0 & 0 & 0 & 1 \\ 0 & 0 & 1 & 0 \end{pmatrix} \begin{pmatrix} \alpha \\ \beta \\ \gamma \\ \delta \end{pmatrix} = \begin{pmatrix} \beta \\ \alpha \\ \delta \\ \gamma \end{pmatrix}, \tag{B.9}$$

which means that the amplitude of the states $|00\rangle$ and $|01\rangle$ has been interchanged, as well as for the states $|10\rangle$ and $|11\rangle$.

Note that the order in which the operators appear affect the final result. To put first the NOT gate and then the identity gate would have negated the first qubit.

B.1.5 The controlled NOT gate

This is a very useful two-qubit gate that cannot be factorized and nevertheless meets the requierement of unicity.

The funcion of the controlled NOT (CNOT) gate is very simple: if the control qubit is in the state $|1\rangle$, the second qubit will be negated. For example, if the system is in the state $|00\rangle + |10\rangle$ and the control qubit is the first one, the system would be changed into $|00\rangle + |11\rangle$. In matrix representation, this is:

$$\mathbf{CNOT}_1 = \begin{pmatrix} 1 & 0 & 0 & 0 \\ 0 & 1 & 0 & 0 \\ 0 & 0 & 0 & 1 \\ 0 & 0 & 1 & 0 \end{pmatrix}. \tag{B.10}$$

The control qubit could also be the second one:

$$\mathbf{CNOT}_2 = \begin{pmatrix} 1 & 0 & 0 & 0 \\ 0 & 0 & 0 & 1 \\ 0 & 0 & 1 & 0 \\ 0 & 1 & 0 & 0 \end{pmatrix}. \tag{B.11}$$

The CNOT gate is very important because it can be used along with

the Hadamard gate to prepare an entangled states from the $|00\rangle$ state.

$$(\mathbf{CNOT}_2)(\mathbf{I}\otimes\mathbf{H})(|00\rangle) \tag{B.12}$$

$$\begin{pmatrix} 1 & 0 & 0 & 0 \\ 0 & 0 & 0 & 1 \\ 0 & 0 & 1 & 0 \\ 0 & 1 & 0 & 0 \end{pmatrix} \frac{1}{\sqrt{2}} \left(\begin{pmatrix} 1 & 0 \\ 0 & 1 \end{pmatrix} \otimes \begin{pmatrix} 1 & 1 \\ 1 & -1 \end{pmatrix} \right) \begin{pmatrix} 1 \\ 0 \\ 0 \\ 0 \end{pmatrix} \tag{B.13}$$

$$\begin{pmatrix} 1 & 0 & 0 & 0 \\ 0 & 0 & 0 & 1 \\ 0 & 0 & 1 & 0 \\ 0 & 1 & 0 & 0 \end{pmatrix} \begin{pmatrix} 1\begin{pmatrix} 1 & 1 \\ 1 & -1 \end{pmatrix} & 0\begin{pmatrix} 1 & 1 \\ 1 & -1 \end{pmatrix} \\ 0\begin{pmatrix} 1 & 1 \\ 1 & -1 \end{pmatrix} & 1\begin{pmatrix} 1 & 1 \\ 1 & -1 \end{pmatrix} \end{pmatrix} \begin{pmatrix} 1/\sqrt{2} \\ 0 \\ 0 \\ 0 \end{pmatrix} \tag{B.14}$$

$$\begin{pmatrix} 1 & 0 & 0 & 0 \\ 0 & 0 & 0 & 1 \\ 0 & 0 & 1 & 0 \\ 0 & 1 & 0 & 0 \end{pmatrix} \begin{pmatrix} 1 & 1 & 0 & 0 \\ 1 & -1 & 0 & 0 \\ 0 & 0 & 1 & 1 \\ 0 & 0 & 1 & -1 \end{pmatrix} \begin{pmatrix} 1/\sqrt{2} \\ 0 \\ 0 \\ 0 \end{pmatrix} \tag{B.15}$$

$$\begin{pmatrix} 1 & 0 & 0 & 0 \\ 0 & 0 & 0 & 1 \\ 0 & 0 & 1 & 0 \\ 0 & 1 & 0 & 0 \end{pmatrix} \begin{pmatrix} 1/\sqrt{2} \\ 1/\sqrt{2} \\ 0 \\ 0 \end{pmatrix} \tag{B.16}$$

$$\begin{pmatrix} 1/\sqrt{2} \\ 0 \\ 0 \\ 1/\sqrt{2} \end{pmatrix} = \mathrm{B}_{00} \tag{B.17}$$

Appendix C

Aplication: Quantum Teleportation

In this scheme, it is possible to transmit quantum information using a quantum channel, specifically, the Entanglement shared between two qubits. This algorithm has no classical equivalent.

Suppose that Bobt has to copy certain secret information, for example, the coefficients of a qubit's state. Retrieving the coefficients would be impossible because he would have to repeatedly make a measurement in order to relate the outcome probability with the state's amplitude. Using quantum teleportation, Bob could send the quantum state to Alice using Entanglement and a classical transmition of information.

As input, Bob and Alice share a Bell state (specifically, B_{00}), and the qubit of interest is in the generic state $|\psi\rangle = \alpha|0\rangle + \beta|1\rangle$. The initial state is a combination of the three qubits:

$$|\psi_0\rangle = |\psi\rangle \mathrm{B}_{00} = \frac{1}{\sqrt{2}}[\alpha|0\rangle(|00\rangle + |11\rangle) + \beta|1\rangle(|00\rangle + |11\rangle)] \tag{C.1}$$

where the first two qubits are Bob's, and the third is Alice's. Bob applies a CNOT gate to his two qubits and now has

$$|\psi_1\rangle = \frac{1}{\sqrt{2}}[\alpha|0\rangle(|00\rangle + |11\rangle) + \beta|1\rangle(|10\rangle + |01\rangle)] \tag{C.2}$$

then, he applies a Hadamard gate over the first qubit:

$$|\psi_2\rangle = \frac{1}{2}[\alpha(|0\rangle + |1\rangle)(|00\rangle + |11\rangle) + \beta(|0\rangle - |1\rangle)(|10\rangle + |01\rangle)]. \tag{C.3}$$

This last state can be rewritten as

$$|\psi_2\rangle = 1/2[\alpha(|0\rangle + |1\rangle)(|00\rangle + |11\rangle) + \beta(|0\rangle - |1\rangle)(|10\rangle + |01\rangle)] \tag{C.4}$$

$$=\frac{1}{2}[\alpha(|000\rangle + |011\rangle + |100\rangle + |111\rangle) + \beta(|010\rangle + |001\rangle - |110\rangle - |101\rangle)] \tag{C.5}$$

$$=\frac{1}{2}[\alpha|000\rangle + \beta|001\rangle + \alpha|011\rangle + \beta|010\rangle + \alpha|100\rangle - \beta|101\rangle + \alpha|111\rangle - \beta|110\rangle] \tag{C.6}$$

$$=\frac{1}{2}[|00\rangle(\alpha|0\rangle + \beta|1\rangle) + |01\rangle(\alpha|1\rangle + \beta|0\rangle) + |10\rangle(\alpha|0\rangle - \beta|1\rangle) + |11\rangle(\alpha|1\rangle - \beta|0\rangle)] \tag{C.7}$$

The last expression can be seen as four different states. Notably, the last qubit has already the information of the target qubit. The last thing that Bob has to do es measure his two qubits. If the result is the state $|00\rangle$, Alice has nothing to do, but if the state is one of the other three, Bob has to tell Alice (classically) what is the result state so she can apply an extra operation in order for her to finally retrieve the coefficients of $|\psi\rangle$. From Bob's measurements:

$$\begin{array}{l} 00 \rightarrow |\psi_3(00)\rangle \equiv [\alpha|0\rangle + \beta|1\rangle] \\ 01 \rightarrow |\psi_3(01)\rangle \equiv [\alpha|1\rangle + \beta|0\rangle] \\ 10 \rightarrow |\psi_3(10)\rangle \equiv [\alpha|0\rangle - \beta|1\rangle] \\ 11 \rightarrow |\psi_3(11)\rangle \equiv [\alpha|1\rangle - \beta|0\rangle] \end{array} \tag{C.8}$$

If Bob obtains the state $|\psi_3(01)\rangle$, Alice has to apply the $\mathbf{X}$ gate; if the $|\psi_3(10)\rangle$ state is measured, Alice has to apply the $\mathbf{Z}$ gate and finally, if Bob measures the state $|\psi_3(11)\rangle$ then it is necessary to use first $\mathbf{Z}$ and then $\mathbf{X}$.

C.1 Quantum teleportation with matrices

As an exercise, we can repeat the quantum teleportation example in matrix form. The input is

$$|\psi_0\rangle = |\psi\rangle \otimes |\mathrm{B}_{00}\rangle = \frac{1}{\sqrt{2}} \begin{pmatrix} \alpha \begin{pmatrix} 1 \\ 0 \\ 0 \\ 1 \end{pmatrix} \\ \beta \begin{pmatrix} 1 \\ 0 \\ 0 \\ 1 \end{pmatrix} \end{pmatrix} = \frac{1}{\sqrt{2}} \begin{pmatrix} \alpha \\ 0 \\ 0 \\ \alpha \\ \beta \\ 0 \\ 0 \\ \beta \end{pmatrix}. \tag{C.9}$$

Now we need a three qubit gate, with $\mathbf{CNOT}_1$ acting on the first two,

$$\mathbf{CNOT}_1 \otimes \mathbf{I} = \begin{pmatrix} 1 & 0 & 0 & 0 \\ 0 & 1 & 0 & 0 \\ 0 & 0 & 0 & 1 \\ 0 & 0 & 1 & 0 \end{pmatrix} \otimes \begin{pmatrix} 1 & 0 \\ 0 & 1 \end{pmatrix} \tag{C.10}$$

$$= \begin{pmatrix} 1\begin{pmatrix} 1 & 0 \\ 0 & 1 \end{pmatrix} & 0\begin{pmatrix} 1 & 0 \\ 0 & 1 \end{pmatrix} & 0\begin{pmatrix} 1 & 0 \\ 0 & 1 \end{pmatrix} & 0\begin{pmatrix} 1 & 0 \\ 0 & 1 \end{pmatrix} \\ 0\begin{pmatrix} 1 & 0 \\ 0 & 1 \end{pmatrix} & 1\begin{pmatrix} 1 & 0 \\ 0 & 1 \end{pmatrix} & 0\begin{pmatrix} 1 & 0 \\ 0 & 1 \end{pmatrix} & 0\begin{pmatrix} 1 & 0 \\ 0 & 1 \end{pmatrix} \\ 0\begin{pmatrix} 1 & 0 \\ 0 & 1 \end{pmatrix} & 0\begin{pmatrix} 1 & 0 \\ 0 & 1 \end{pmatrix} & 0\begin{pmatrix} 1 & 0 \\ 0 & 1 \end{pmatrix} & 1\begin{pmatrix} 1 & 0 \\ 0 & 1 \end{pmatrix} \\ 0\begin{pmatrix} 1 & 0 \\ 0 & 1 \end{pmatrix} & 0\begin{pmatrix} 1 & 0 \\ 0 & 1 \end{pmatrix} & 1\begin{pmatrix} 1 & 0 \\ 0 & 1 \end{pmatrix} & 0\begin{pmatrix} 1 & 0 \\ 0 & 1 \end{pmatrix} \end{pmatrix} \tag{C.11}$$

$$= \begin{pmatrix} 1 & 0 & 0 & 0 & 0 & 0 & 0 & 0 \\ 0 & 1 & 0 & 0 & 0 & 0 & 0 & 0 \\ 0 & 0 & 1 & 0 & 0 & 0 & 0 & 0 \\ 0 & 0 & 0 & 1 & 0 & 0 & 0 & 0 \\ 0 & 0 & 0 & 0 & 0 & 0 & 1 & 0 \\ 0 & 0 & 0 & 0 & 0 & 0 & 0 & 1 \\ 0 & 0 & 0 & 0 & 1 & 0 & 0 & 0 \\ 0 & 0 & 0 & 0 & 0 & 1 & 0 & 0 \end{pmatrix}. \tag{C.12}$$

Applying the gate:

$$\begin{pmatrix} 1 & 0 & 0 & 0 & 0 & 0 & 0 & 0 \\ 0 & 1 & 0 & 0 & 0 & 0 & 0 & 0 \\ 0 & 0 & 1 & 0 & 0 & 0 & 0 & 0 \\ 0 & 0 & 0 & 1 & 0 & 0 & 0 & 0 \\ 0 & 0 & 0 & 0 & 0 & 0 & 1 & 0 \\ 0 & 0 & 0 & 0 & 0 & 0 & 0 & 1 \\ 0 & 0 & 0 & 0 & 1 & 0 & 0 & 0 \\ 0 & 0 & 0 & 0 & 0 & 1 & 0 & 0 \end{pmatrix} \frac{1}{\sqrt{2}} \begin{pmatrix} \alpha \\ 0 \\ 0 \\ \alpha \\ \beta \\ 0 \\ 0 \\ \beta \end{pmatrix} = \begin{pmatrix} \alpha \\ 0 \\ 0 \\ \alpha \\ 0 \\ \beta \\ \beta \\ 0 \end{pmatrix}. \tag{C.13}$$

Now, another three-qubit gate is needed with the Hadamard gate acting

on the first qubit:

$$H \otimes I \otimes I = \frac{1}{\sqrt{2}} \begin{pmatrix} 1 & 1 \\ 1 & -1 \end{pmatrix} \otimes \begin{pmatrix} 1 & 0 \\ 0 & 1 \end{pmatrix} \otimes \begin{pmatrix} 1 & 0 \\ 0 & 1 \end{pmatrix} \tag{C.14}$$

$$= \frac{1}{\sqrt{2}} \begin{pmatrix} 1 & 0 & 1 & 0 \\ 0 & 1 & 0 & 1 \\ 1 & 0 & -1 & 0 \\ 0 & 1 & 0 & -1 \end{pmatrix} \otimes \begin{pmatrix} 1 & 0 \\ 0 & 1 \end{pmatrix} \tag{C.15}$$

$$= \frac{1}{\sqrt{2}} \begin{pmatrix} 1 & 0 & 0 & 0 & 1 & 0 & 0 & 0 \\ 0 & 1 & 0 & 0 & 0 & 1 & 0 & 0 \\ 0 & 0 & 1 & 0 & 0 & 0 & 1 & 0 \\ 0 & 0 & 0 & 1 & 0 & 0 & 0 & 1 \\ 1 & 0 & 0 & 0 & -1 & 0 & 0 & 0 \\ 0 & 1 & 0 & 0 & 0 & -1 & 0 & 0 \\ 0 & 0 & 1 & 0 & 0 & 0 & -1 & 0 \\ 0 & 0 & 0 & 1 & 0 & 0 & 0 & -1 \end{pmatrix}, \tag{C.16}$$

Finally, applying the gate,

$$\frac{1}{\sqrt{2}} \begin{pmatrix} 1 & 0 & 0 & 0 & 1 & 0 & 0 & 0 \\ 0 & 1 & 0 & 0 & 0 & 1 & 0 & 0 \\ 0 & 0 & 1 & 0 & 0 & 0 & 1 & 0 \\ 0 & 0 & 0 & 1 & 0 & 0 & 0 & 1 \\ 1 & 0 & 0 & 0 & -1 & 0 & 0 & 0 \\ 0 & 1 & 0 & 0 & 0 & -1 & 0 & 0 \\ 0 & 0 & 1 & 0 & 0 & 0 & -1 & 0 \\ 0 & 0 & 0 & 1 & 0 & 0 & 0 & -1 \end{pmatrix} \frac{1}{\sqrt{2}} \begin{pmatrix} \alpha \\ 0 \\ 0 \\ \alpha \\ 0 \\ \beta \\ \beta \\ 0 \end{pmatrix} \tag{C.17}$$

$$= \frac{1}{2} \begin{pmatrix} \alpha \\ \beta \\ \beta \\ \alpha \\ \alpha \\ -\beta \\ -\beta \\ \alpha \end{pmatrix} \rightarrow \begin{pmatrix} 000 \\ 001 \\ 010 \\ 011 \\ 100 \\ 101 \\ 110 \\ 111 \end{pmatrix} \tag{C.18}$$

This last vector is equivalent to eq. (C.6).

Appendix D

Application: Dense coding

In this scheme, it is possible to use the transmission of one qubit in order to obtain two classical bits. The concept is simple, two qubits are had in the Bell state B_{00}, with the first qubit the one to be transmitted. This qubit can be manipulated in such a way that the two qubit system changes into any of the other Bell states (or remains unchanged). Bell states are orthogonal between them, so it is possible, in principle, to build measurment operators that can distinguish them. Each of the four Bell states correspond to a two classical bit string.

The operations are:

$$(\mathbf{I}\otimes\mathbf{I})(\mathrm{B}_{00})\rightarrow\mathrm{B}_{00} \tag{D.1}$$
$$(\mathbf{Z}\otimes\mathbf{I})(\mathrm{B}_{00})\rightarrow\mathrm{B}_{01} \tag{D.2}$$
$$(\mathbf{X}\otimes\mathbf{I})(\mathrm{B}_{00})\rightarrow\mathrm{B}_{10} \tag{D.3}$$
$$(i\mathbf{Y}\otimes\mathbf{I})(\mathrm{B}_{00})\rightarrow\mathrm{B}_{11}, \tag{D.4}$$

with i the imaginary unit and the $\mathbf{Y}$ gate defined as

$$\mathbf{Y}\equiv\begin{pmatrix}0 & -i\\ i & 0\end{pmatrix}. \tag{D.5}$$

The set of gates $\mathbf{I},\mathbf{X},\mathbf{Y}$ and $\mathbf{Z}$ are called *Pauli matrices*.

The operator for measuring the state B_{00} is simply

$$\begin{aligned} M_{\mathrm{B}_{00}} &\equiv \left(\frac{|00\rangle+|11\rangle}{\sqrt{2}}\right)\left(\frac{\langle 00|+\langle 11|}{\sqrt{2}}\right)\\ &\equiv \frac{1}{2}\left(|00\rangle\langle 00|+|00\rangle\langle 11|+|11\rangle\langle 00|+|11\rangle\langle 11|\right)\\ &\equiv \frac{1}{2}\begin{pmatrix}1&0&0&1\\0&0&0&0\\0&0&0&0\\1&0&0&1\end{pmatrix} \end{aligned} \tag{D.6}$$

Appendix E

Published Paper

IOP PUBLISHING JOURNAL OF PHYSICS A: MATHEMATICAL AND THEORETICAL

J. Phys. A: Math. Theor. **42** (2009) 315302 (14pp) doi:10.1088/1751-8113/42/31/315302

Designing lattice structures with maximal nearest-neighbor entanglement

J C Navarro-Muñoz[1], R López-Sandoval[1] and M E García[2]

[1] Instituto Potosino de Investigación Científica y Tecnológica, Camino a la presa San José 2055, 78216 San Luis Potosí, Mexico

[2] Theoretische Physik, FB 18, Universität Kassel and Center for Interdisciplinary Nanostructure Science and Technology (CINSaT), Heinrich-Plett-Str.40, 34132 Kassel, Germany

Received 4 March 2009, in final form 8 May 2009
Published 15 July 2009
Online at stacks.iop.org/JPhysA/42/315302

Abstract

In this paper, we study the numerical optimization of nearest-neighbor concurrence of bipartite one- and two-dimensional lattices, as well as non-bipartite two-dimensional lattices. These systems are described in the framework of a tight-binding Hamiltonian while the optimization of concurrence was performed using genetic algorithms. Our results show that the concurrence of the optimized lattice structures is considerably higher than that of non-optimized systems. In the case of one-dimensional chains, the concurrence increases dramatically when the system begins to dimerize, i.e., it undergoes a structural phase transition (Peierls distortion). This result is consistent with the idea that entanglement is maximal or shows a singularity near quantum phase transitions. Moreover, the optimization of concurrence in two-dimensional bipartite and non-bipartite lattices is achieved when the structures break into smaller subsystems, which are arranged in geometrically distinguishable configurations.

PACS numbers: 03.67.−a, 03.65.Ud, 73.43.Nq, 71.10.Fd

1. Introduction

Quantum entanglement is one of the most distinctive features in quantum mechanics, yet its properties are still not fully understood. This quantum resource is considered a key element of several quantum information and quantum computation proposals such as quantum teleportation [1], superdense coding [2], certain kinds of quantum key distribution schemes and quantum secret-sharing protocols [3, 4].

Recently, much research has been focused on a better understanding of quantum correlations in multiparticle systems [5–8]. A characteristic property that sets apart quantum correlations (or entanglement) from the classical ones is that entanglement cannot be freely

The last page

All code compiled using a licenced Portland Group Fortran 90 compiler under Linux enviroment. LAPACK routines were also used. Code run on a dual Opteron workstation (“genesis”) and a dual Xeon workstation (“comalli”).

Figures created with GIMP and xmgrace.

Text compiled with LaTeX.